LAPPEENRANTA UNIVERSITY OF TECHNOLOGY
School of Technology
Technical Physics

Kapustin Dmitry

MAGNETIC PROPERTIES OF MULTI-WALLED NANOTUBES ON POLYSTERENE SUBSTRATE

Examiners Professor Erkki Lähderanta

D.Sc. Zakharchuk Ivan

ABSTRACT

Lappeenranta University of Technology

School of Technology

Technical Physics

Kapustin Dmitry

MAGNETIC PROPERTIES OF MULTI-WALLED NANOTUBES ON POLYSTERENE SUBSTRATE

Master's thesis

2014

53 pages, 34 pictures, 2 tables.

Examiners: Professor Erkki Lähderanta

D.Sc Ivan Zakharchuk

Keywords: nanotubes, polysterene substrate, magnetization, magnetic dependence, SQUID magnetometer.

Nanotubes are one of the most perspective materials in modern nanotechologies. It makes present investigation very actual. In this work magnetic properties of multi-walled nanotubes on polystyrene substrate are investigated by using quantum magnetometer SQUID. Main purpose was to obtain magnetic field and temperature dependences of magnetization and to compare them to existing theoretical models of magnetism in carbon-bases structures. During data analysis a mathematical algorithm for obtained data filtration was developed because measurement with quantum magnetometer assume big missives of

number data, which contain accidental errors. Nature of errors is drift of SQUID signal, errors of different parts of measurement station.

Nanotube samples on polystyrene substrate were studied with help of atomic force microscope. On the surface traces of nanotube were found contours, which were oriented in horizontal plane. This feature was caused by rolling method for samples. Detailed comparison of obtained dependences with information of other researches on this topic allows to obtain some conclusions about nature of magnetism in the samples. It emphasizes importance and actuality of this scientific work.

Acknowledgements.

I would like to thank my supervisor, Zakharchuk Ivan, for invaluable help in process of measurement on SQUID magnetometer, detailed acquaintance with all devices in laboratory, help in checking and editing of master thesis project. I would like to thank Professor Erkki Lahderanta for advices in choosing of scientific articles, checking and estimating of my work. Also I thank a lot my parents which support me every time and give wise advices.

Table of contents

Abbreviations and symbols

CNT Carbon nanotube

CVD Chemical vapor deposition

FC Field cooling

SQUID Superconducting Quantum Interference Device

SWCNT Single-walled carbon nanotubes

TEM Transmission electron microscopy

TRM Thermoremanent magnetization

ZFC Zero field cooling

1. Literature overview

1.1. Determination of nanotubes, role of nanotubes in development of modern nanotechnologies

Discovery of nanotubes is one of the most significant discoveries in modern nanotechnology. This form of carbon occupies an intermediate position between graphite and fullerenes. Nanotubes have unique physical properties which cannot be attached to fullerenes or graphite based structures. Big amount of these properties depend on geometrical characteristics of nanotubes.

Nanotube is a cylinder obtained by folding of the hexagonal graphite plane without joints. Mutual orientation of longitudinal nanotube axis and hexagonal graphite plane determine important characteristic called chirality.

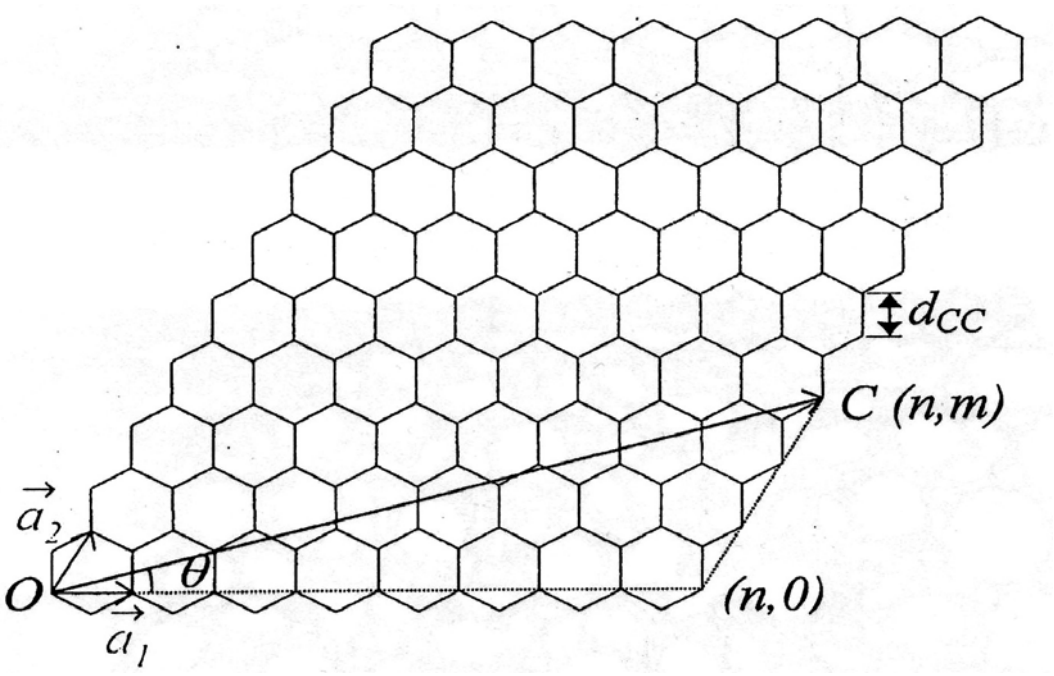

Figure 1.1.1. Chirality vector of nanotubes[1].

Chirality is characterized by indexes m and n, determined by location of hexagon, which must coincide with original hexagon in result of convolution.

Diameter of nanotube and indexes of chirality are connected:

$$D = \sqrt{m^2 + n^2 - mn} \cdot \frac{3 \cdot d_0}{\pi} \quad , \qquad (1.1.1)$$

where d_0 = 0.142 nm is a typical value of distance between carbon atoms.

Depending on the value of chirality indexes different types of nanotubes are distinguish (Figure 1.1.1):

- «armchair» type («n» = «m»);

- «zigzag» type («m» = 0).

Fundamentally classification of geometrical forms of nanotubes is based on orientation of carbon bonds in relation to nanotube axis. Nanotube is «armchair» if all bonds are perpendicular to axis, in opposite way it has name «zigzag» type. But when the bonds are neither perpendicular nor parallel to axis, such nanotubes are called «chiral».

Chirality has influence on electronic properties of nanotubes. For example, nanotubes with indexes of (10, 10) have metal properties. American researchers from University of Clemson have discovered technology of synthesis of such single-layer nanotubes with sequence of special processing stages: chemical and thermal processing [2].

Sp^2 hybridization is one of the basic types of hybridization for carbon structures. Practically it means existence of π-electron which stipulate conductivity of graphite. In case of nanotubes, the type of hybridization can change from sp^2 to sp^3. It is one of the reasons of their unique properties, for example, very high value of mechanical strength.

Nanotubes have some unique features which have wide perspectives in science and technical applications. One of the most important features is big mechanical strength.

Many properties of nanotubes can be explained by investigation of their electronic properties. Significant point in this explanation is the band structure of nanotubes. Typical band structure of nanotubes with different chirality indexes is shown of Figure 1.1.2.

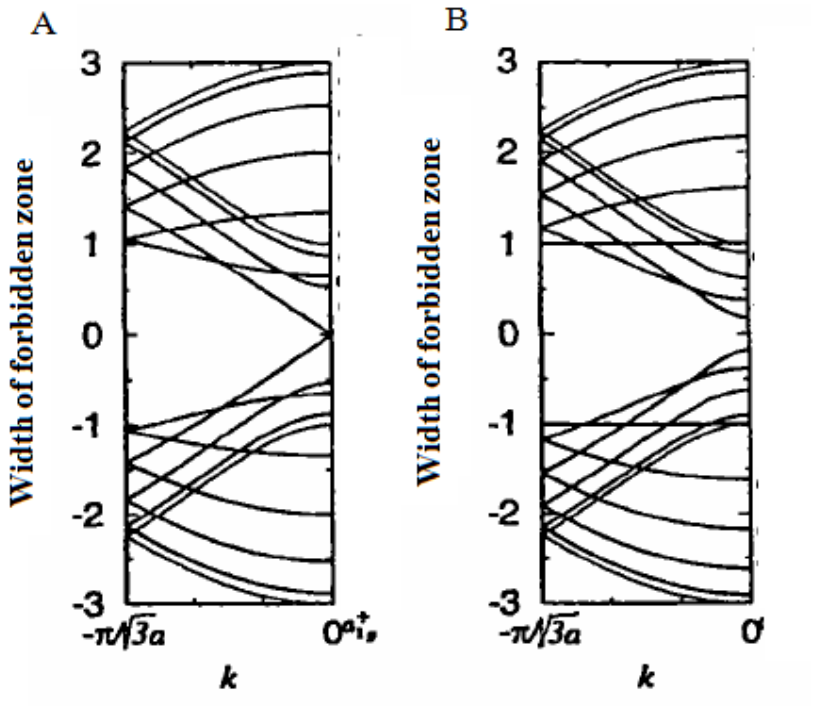

Figure 1.1.2. Band structure for multi-walled nanotubes with different values of chirality indexes (m, n): A) chirality indexes (9, 0), B) hilarity indexes (10, 0) [3].

Figure 1.1.2 shows band structure for nanotubes with different chirality indexes. For the case of nanotube having (9, 0) indexes, valence band and conduction band overlap at zero wave vector, «k» = 0. This means that the nanotube has properties of metal. This property is saved for all nanotubes with «m» index multiple of 3. In Figure 1.1.2, B the existence of an energy gap between two bands leads to semiconductor properties.

Nanotubes have structure based on carbon hexagons. If hexagon changes to pentagon, nanotube bends and all electrical and quantum-mechanical properties change [4].

Nanotube are used as a base structure in field-effect transistors. Structure of such transistor is drawn in Figure 1.1.3.

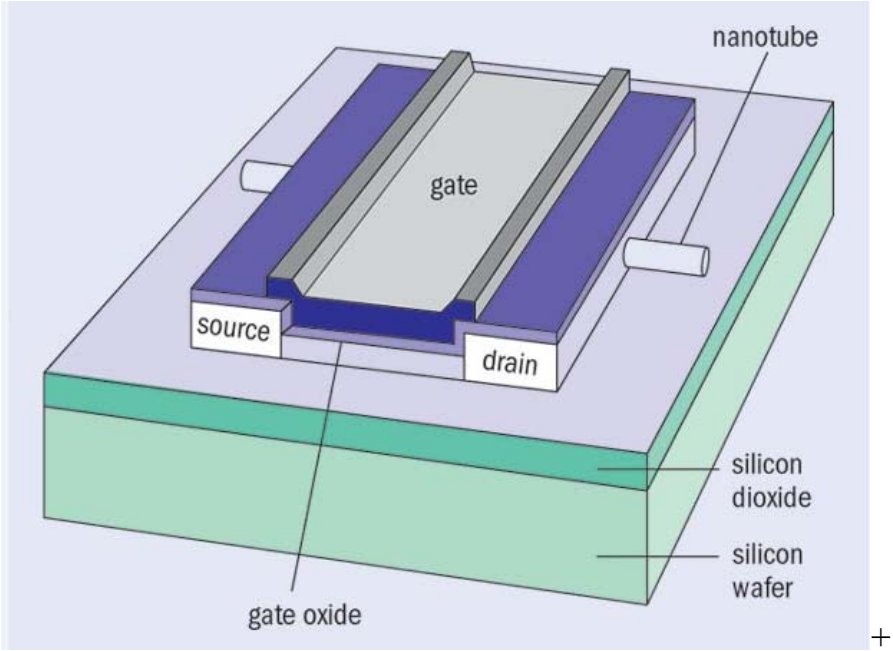

Figure 1.1.3. Structural scheme of transistor based on nanotubes [5].

Principle of such transistor functionality is based on using the nanotube as a channel for charge transfer. There are two conductive rails on silicon substrate, and nanotube is situated between these rails. In simple state nanotube is a good dielectric, but if external electric field is applied, concentration of free charge carries is enhanced, and nanotube becomes a good conductor. Thus change of electric field on the gate allows to control electric properties of the nanotube and the transistor state [6].

A nanotube, connecting two superconductors demonstrates superconductive properties, because Cooper pairs, which are basic charge carriers in superconductors, do not split after passing through nanotube [7]. Use of superconducting wires is perspective in formation of big superconducting systems, quantum magnetometers and in thermo nuclear reactors.

One area of nanotubes applications is «NRAM» memory, developed by company «Nantero». This technology is based on an effect that nanotubes in a matrix can either be touching or slightly separated, depending on their mechanical state. Each NRAM «cell» consists of an interlinked network of CNTs located between two electrodes as illustrated in Figure 1.1.4. The CNT is located between two metal electrodes forms the NRAM cell [8].

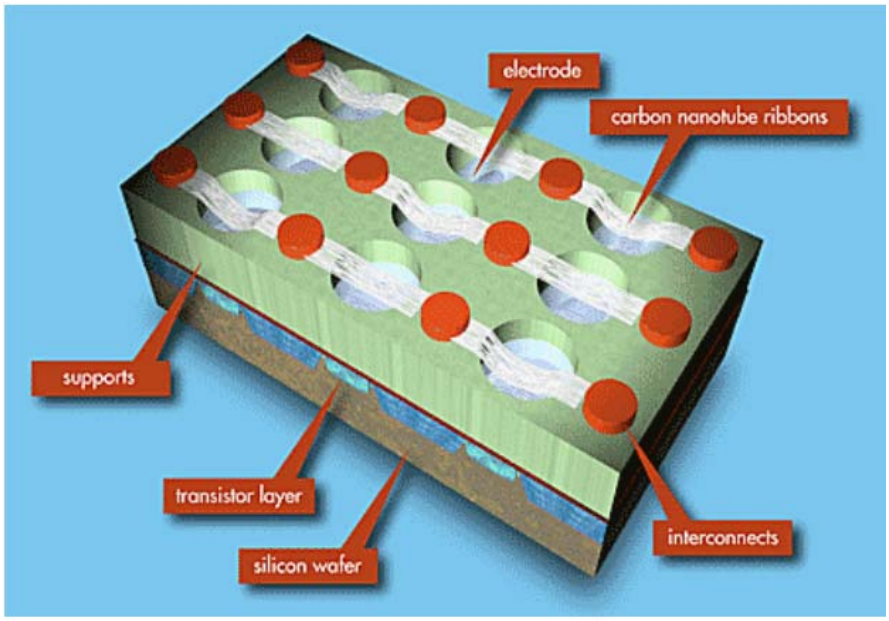

Figure 1.1.4.Memory on nanotubes abstract scheme [9].

In the future nanotubes can be a foundation of all schemes of electronic devices, including modern computer systems. It can result to increasing of information recording density.

1.2 Synthesis of nanotubes.

Problem that exists in manufacturing of nanotubes is in obtaining of desired combination of texture and properties of nanotubes [10]. This has strong connection with used method of synthesis. From historical point of view, first method of synthesis was discovered by Japan scientist Sumio Idjim [11]. At the same time similar method was described in work of Chernozatonsky [12].

First methods of nanotubes synthesis was arc discharge. Evaporation of anode material starts when arc is burning. Finally soot with presence of nanotubes is formed. Typical voltage is 20 V, and value of current is not less than 50 A. The whole process occurs without any catalyst.

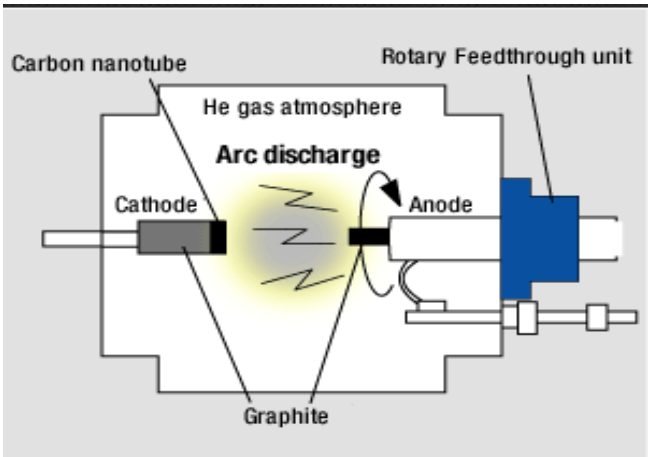

Figure 1.2.1. Technological scheme of arc discharge method to obtain nanotubes [13].

Adding of metal catalyst, for instance, nickel or cobalt, results to formation of only single-wall nanotubes. One of serious disadvantages of such synthesis type is presence of other carbon products in content of evaporated soot. It means that a process of dividing these components is needed.

Second synthesis method is laser ablation. Basic parts of technological scheme are drawn in Figure 1.2.2: pulsed laser, graphite target, heater and collector. Target material is evaporated by laser and the evaporated particles deposit on collector surface in flow of inert gases. Structural properties strongly depend on

temperature. Like in previous method, addition of catalyst materials increases percentage of formed single-wall nanotubes. One of significant advantages of laser ablation is high level of structural perfection and purity of nanotubes.

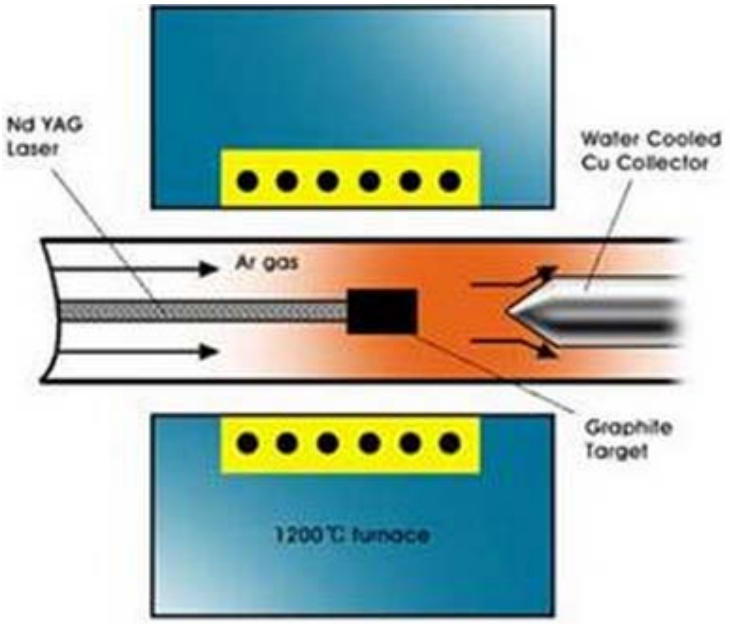

Figure 1.2.2. Scheme of laser ablation method [14].

One of the most widely used methods of nanotubes synthesis is plasma-enchanted vapour deposition (CVD).

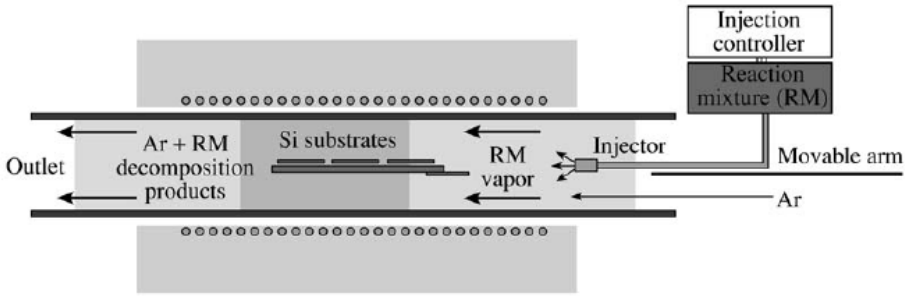

Figure 1.2.3.Scheme of a CVD reactor used for growth of aligned CNT arrays [15].

During CVD, a substrate is prepared with a layer of metal catalyst particles, most commonly nickel or cobalt. The metal nanoparticles can also be produced by other

ways, including reduction of oxides or oxides solid solutions [16]. The diameters of the nanotubes that are to be grown are related to the size of the metal particles. The substrate is heated to approximately 700°C.

To initiate the growth of nanotubes, two gases are bled into the reactor: a process gas (ammonia, nitrogen or hydrogen) and a carbon-containing gas (acetylene or ethylene,). Nanotubes grow at the sites of the metal catalyst; the carbon-containing gas is broken apart at the surface of the catalyst particle, and the carbon is transported to the edges of the particle, where it forms the nanotubes. The catalyst particles can stay at the tips of the growing nanotube during growth, or remain at the nanotube base, depending on the adhesion between the catalyst particle and the substrate.

1.3. Types of magnetism for solids

Five different types of magnetism exist: diamagnetism, paramagnetism, ferromagnetism, antiferromagnetism and ferrimagnetism. The main reason of different magnetic properties of solids is arrangement and interaction of magnetic moments. Additionally diamagnetic property of electron shell and paramagnetic property of conduction electrons have influence on magnetic arrangement in solids.

Basically magnetic ordering is a result of balance of thermal movement and arranging factor caused by magnetic forces. These define two types of magnetism: non-cooperative, when different ions do not interact, and cooperative when such interactions is exist.

Diamagnetism is a magnetic property caused by induction of current on electronic shells in atoms. Practically it assumes appearance of magnetic moments ordered opposite to the direction of external magnetic field.In diamagnetic materials absence of external magnetic field means that magnetic moments of all atoms are compensated. When magnetic field is applied, atoms have induced magnetic moments oriented opposite to the direction of field.

Vector of magnetization for diamagnetic materials can be calculated using Equation 1.3.1:

$$\bar{J} = \frac{n \cdot \Delta \bar{P}_m}{\Delta V} = n_0 \cdot \overline{\Delta P_m} = \frac{\bar{B}}{\mu_0} \cdot \chi = \bar{H} \cdot \chi \ , \qquad (1.3.1)$$

where n_0 is concentration of atoms, μ_0 is magnetic constant, χ is magnetic susceptibility of medium, ΔV is elementary volume of isotropic magnetic material, and $\Delta \bar{P}_m$ is magnetically induced moments of atom.

Main features of diamagnetism are non-cooperative character of magnetic ordering and negative magnetic susceptibility.

Paramagnetism is magnetism appearing when ions in solid have spontaneous magnetic moments. Paramagnet is magnetized to direction of external magnetic

field, and full magnetization of material consists of two components: external magnetic field component and a component caused by induced internal field. In t absence of external magnetic field, vectors of magnetization of atoms are oriented randomly.

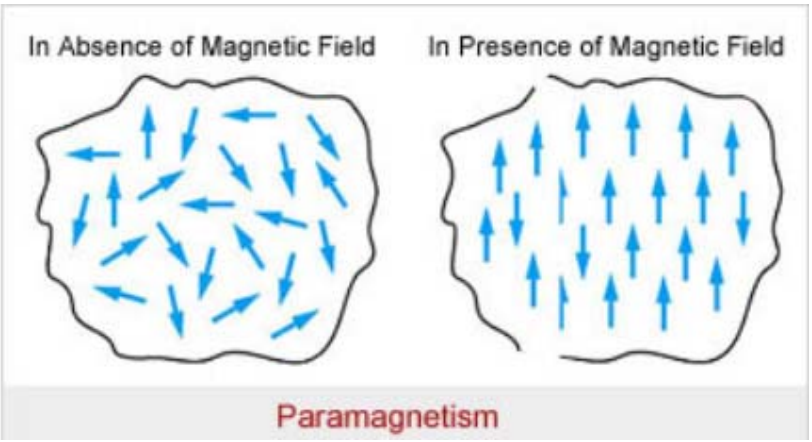

Figure 1.3.1. Orientation of magnetic vectors of atoms for paramagnetic materials [17].

Ferromagnetism is cooperative type magnetism, characterized by magnetization existing even if external magnetic field is not applied. For ideal ferromagnetic materials all ions have equal spontaneous magnetic moments.

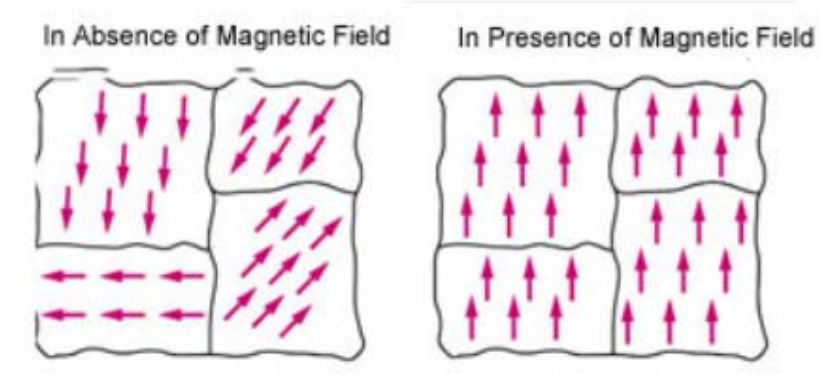

Figure 1.3.2. Orientation of magnetic vectors of atoms for feromagnetic material [18].

When magnetic field is applied, ferromagnetic material is partitioned into domains, small regions magnetized, as shown in Figure 1.3.2. This is caused by minimization of magnetostatic energy.

Magnetization curve of ferromagnetic material is shown in Figure 1.3.3.

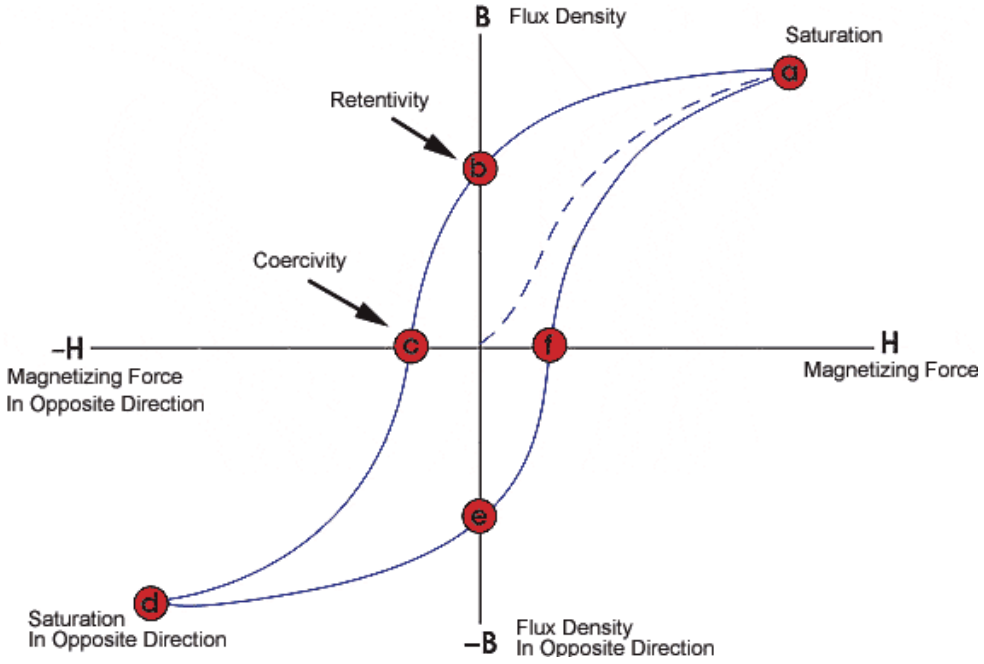

Figure 1.3.3.Magnetisation curve for ferromagnetic materials [19].

In Figure 1.3.3 is shown coercivity, remanent magnetization and saturation. The loop is generated by measuring the magnetic flux of a ferromagnetic material while the magnetizing force is changed [20].

A ferromagnetic material that has not been previously magnetized or has been thoroughly demagnetized will follow the dashed line as «H» is increased.

At point «a» almost all of the magnetic domains are aligned and an additional increase in the magnetizing force will produce very little increase in magnetic flux. The material has reached the point of magnetic saturation. When «H» is reduced to zero, the curve will move from point «a» to point «b».

This is referred to as the point of remanence the graph and indicates the remanence or level of residual magnetism in the material. In this point some of the magnetic domains remain aligned but some have lost their alignment. As the magnetizing force is reversed, the curve moves to point «c», where the flux is reduced to zero. This is called the point of coercivity on the curve. Here the reversed magnetizing

force has flipped enough of the domains so that the net flux within the material is zero. The force required to remove the residual magnetism from the material is called the coercive force or coercivity of the material.

As the magnetizing force is increased in the negative direction, the material will again become magnetically saturated but in the opposite direction (point "d"). Reducing «H» to zero brings the curve to point «e». It will have a level of residual magnetism equal to that achieved in the other direction. Increasing «H» back in the positive direction will return «B» to zero. The curve does not return to the origin of the graph because some force is required to remove the residual magnetism. The curve will take a different path from point «f» back to the saturation point where it completes the loop.

Remanence is a measure of the residual flux density corresponding to the saturation induction of a magnetic material. The value of «B» at point «b» in Figure 1.3.3 on the hysteresis curve corresponds to remanence.

Residual magnetism or residual flux is the magnetic flux density that remains in a material when the magnetizing force is zero. Residual magnetism and remanence are the same when the material has been magnetized to the saturation point. However, the level of residual magnetism may be lower than the remanence value if the magnetizing force has not reached the saturation level.

Coercive force is an amount of reverse magnetic field which must be applied to a magnetic material to make the magnetic flux return to zero. In Figure 1.3.3 it is the value of «H» at point «c» on the hysteresis curve.

Permeability, μ is measure of the ability of a substance to sustain a magnetic field, equal to the ratio between magnetic flux density and magnetic field strength. Reluctance is opposition that a ferromagnetic material shows to the establishment of a magnetic field. Reluctance is analogous to the resistance in an electrical circuit.

For explanation of ferromagnetism special model of interaction between magnetic ions and electrons exists. In cases when concentration of magnetic ions is large, effect of grouped electrons ordering starts to influence on magnetic properties. Foundation of this effect is interaction of magnetic ions shells and formation of energy bands. In this case all electrons are delocalized. Magnetism of grouped electronics is a result of interaction between processes, characterized by coupling interaction energy and kinetic energy of electrons [21].

Level of localization get higher with reducing of energy zone for electrons. In case when width of the energy band is compared with energy of coupling interaction, ion acquires its own magnetic moment due to orientation of electron spins. It leads to appearance of delocalized group of electrons with own orientation of spins and new type of magnetic ordering: ferromagnetism and antiferromagnetism . For these types of magnetism coupling interaction energy reduces due to increase of kinetic energy of magnetic electrons.

Evidence for these arguments is band magnetism theory of grouped electrons. In this model all states of electrons split into 2 bands. In bands, electrons have opposite spins and the displacement of bands as seen in Figure 1.3.4.

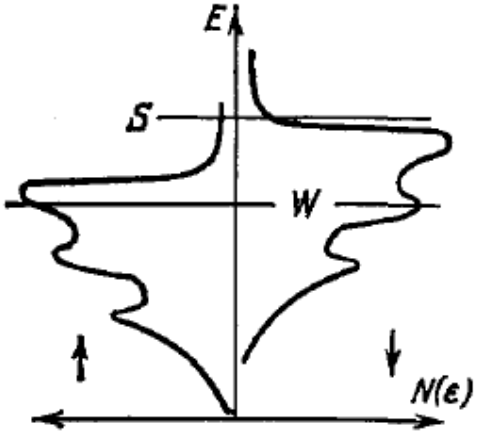

Figure 1.3.4. Distribution of density of energy states for ferromagnetic materials [22].

One criteria of ferromagnetic state existence is presented in Equation 1.3.2:

$$I \cdot N(E_F) > 1 \ , \qquad (1.3.2):$$

where $N(E_F)$ is density of states on Fermi level. Ferromagnetism occurs because the amount of electrons with spins oriented up and amount of electrons with spins oriented down in Figure 1.3.4 are not equal.

1.4. Magnetic properties of nanotubes.

For carbon-based compositions basic type of magnetism is ferromagnetic ordering of spins. Magnetic properties of nanotubes are determined by spin polarization and circular currents, surrounding the nanotube.

Fundamental model, which is used for describing the magnetism in nanotubes is a model of complex magnetic susceptibility. This model considers diamagnetic contribution of different nature, according to Equation 1.4.1.

$$\chi_{total} = \chi_{core} + \chi_P + \chi_L + \chi_{orb} + \chi_c + \chi_{vv} , \qquad (1.4.1)$$

where is χ_{core} is magnetism of magnetic atomic frames, χ_P is paramagnetism Pauli, χ_L is paramagnetsm of Landau, χ_{orb} is coefficient, determined by orbital diamagnetic interactions.

Basically, bulk carbon has magnetic properties which are close to diamagnetism. For the most part of carbon-based structures, the existence of different paramagnetic properties are connected with presence of oxygen and inner structure defects.

According to experimental results magnetism in nanotubes is based on defects. The most common defects are adatoms and vacancies. Appearing of magnetic moment is connected to dangled bonds, which initiate magnetic moment value near 1 μ_B [23]. Electron-electron interaction formes magnetic moment near vacancy. Vacancy can work as a donor site, meaning positive charge accumulation near vacancy. When impurity atom is added, process of charge accumulation can be significantly reduced. It results in limitation of mobility of charge carriers [24].

These are some theories, which can explain nature of magnetism in solids. Several scenarios are available for explanation: bulk, induced, and atomic-scale types of magnetism. From the point of view of electronic properties, all carbon-based structures are divided into nitrogen-carbon compositions, graphite-diamond structures and hydrogen-doped ferromagnetic diamonds.

Foundation of appearing of magnetic effects in carbon-bases structures can be:

1) Fraction of the fullerene cages can brake and unpaired electrons can exist
2) Shape of structure bonds changes due to special transformations
3) Existence of unpaired electrons as a interstructure links

McChonell model describes features of ferromagnetism existence in carbon-based structures is. Basic assumption is that the acceptor and donor sites are assigned to molecules of different kinds. Such vacancy defects play role of donor molecules and defects of another type play role of the acceptor molecules. In this case the ferromagnetism depends on the ability of the defects to create electric fields which bind the charge in the atoms around the defects [25].

Existence of paramagnetic properties in nanotubes was explained in Kvyatslovskii model [26]. Main principle of this model is demonstrated below:

paramagnetic dopant A + diamagnetic fullerene C_{60} —>diamagnetic dopant ion A+ + paramagnetic fullerene ion C_{60}

In this model, the presence of some paramagnetic impurities in fullerene matrix (e. g. hydrogen, fluorine, as well as carbon from partially destroyed fullerenes) leads to a formation of the the paramagnetic fullerene ions C_{60}.These ions have paramagnetic contribution when external magnetic field is applied.
Nanotubes can exhibit superconducting properties. Researchers Zhao and Wang have some experimental evidence of superconductivitinh properties of nanotubes: for instance, superconducting transition or excitation gaps, which can appear in multi-walled nanotubes [27].

In case of thin nanotubes it is possible to observe the diamagnetic Meissner effect [28]. This effect can be isolated successfully only when external magnetic field is parallel to tubes axis. In orientation Meissner effect can be overcome by effects connected with orbital diamagnetic susceptibility.

1.5. SQUID magnetometer.

SX600 Quantum Magnetometer, which was used in experimental part of the work, consists of the following parts:

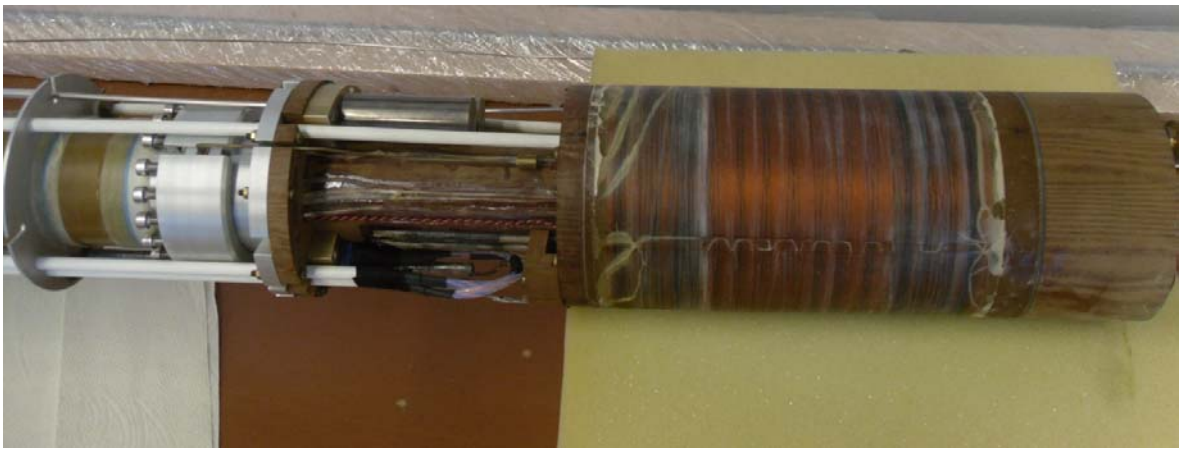

Figure 1.5.1.Solenoid of SQUID magnetometer.

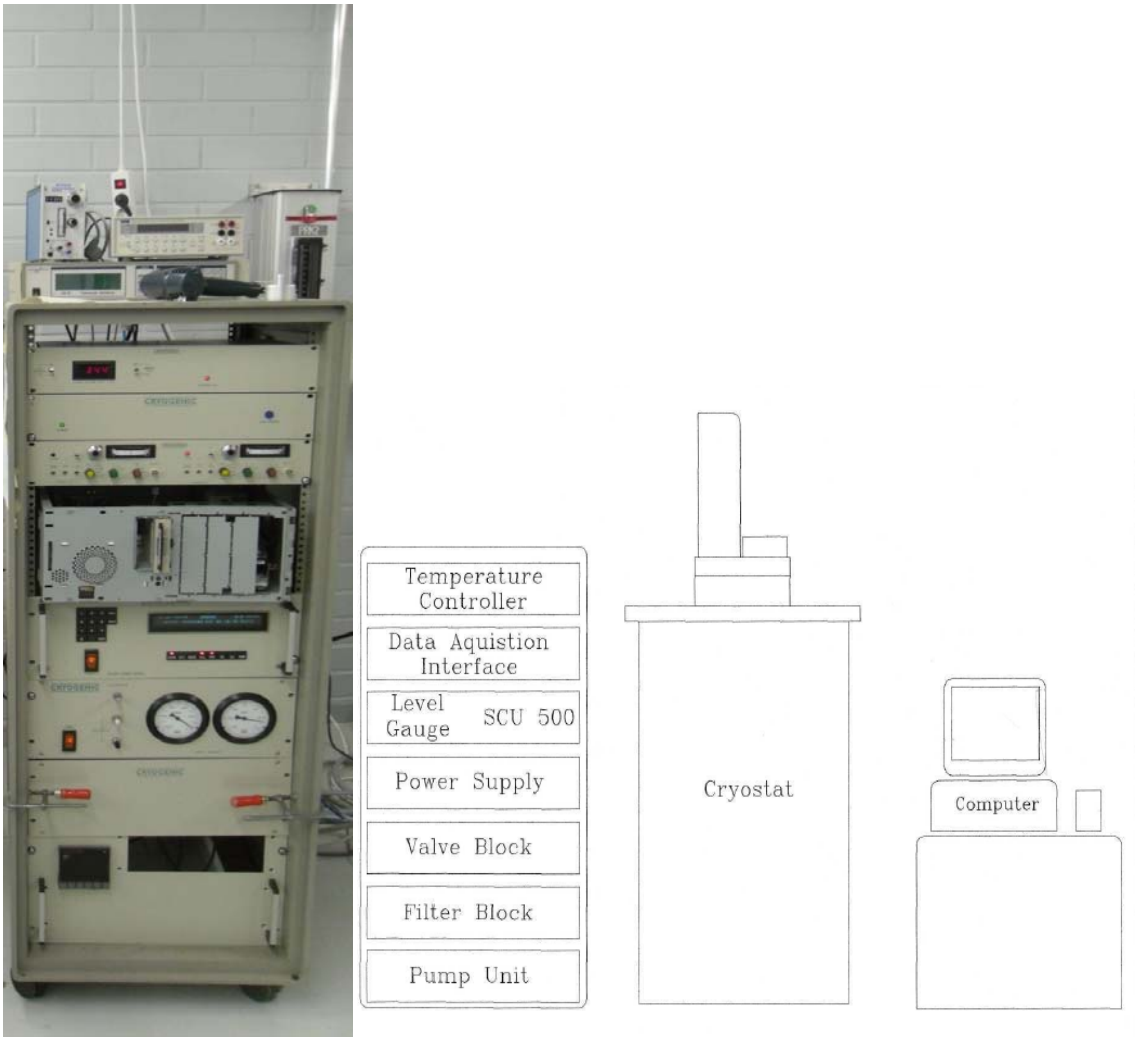

Figure 1.5.2. Blocks of level gauge (left), main blocks of temperature controller (right).

Low temperature parts of measurement station consists of superconducting components: superconducting magnet, detection coil, SQUID system connected to detection coil and external magnetic shield.

The superconducting quantum interference device, SQUID, consist of two superconductors separated by thin insulating layers forming two parallel Josephson junctions. The device is configured as a magnetometer to detect incredibly small magnetic fields: small enough to measure the magnetic fields in living organisms.

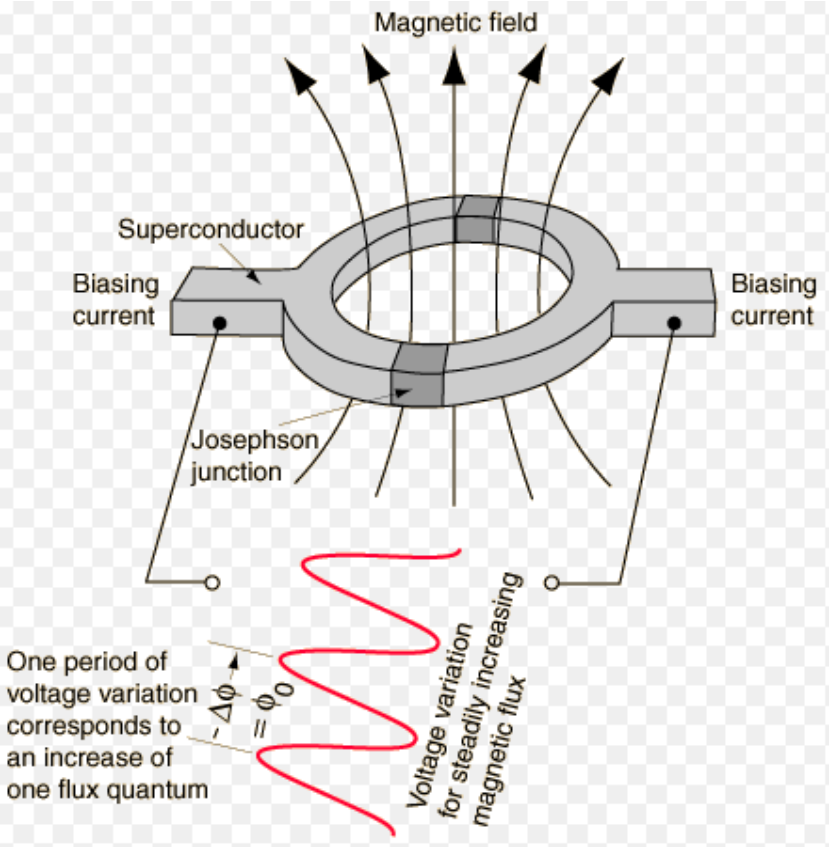

Figure 1.5.3 Josephson junctions in SQUID device [29].

Josephson effect is based on tunneling which is shown in Figure 1.5.4.

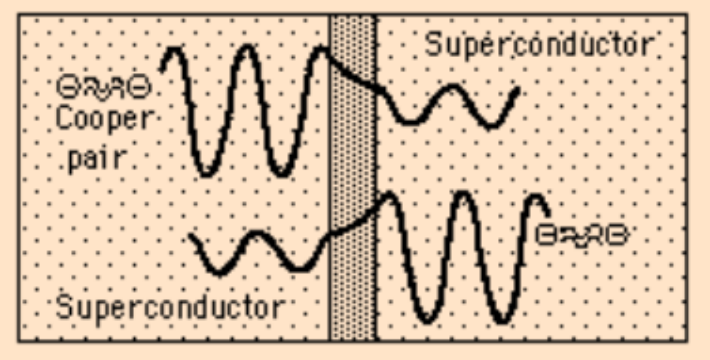

Figure 1.5.4 Scheme of Josephson junction [30].

The wavefunction which describes a Cooper pair of electrons in a superconductor is like free particle with wave function. In fact, all Cooper pairs in a superconductor can be described by a single wave function in the absence of

current because all the pairs have the same phase: they are said to be «phase coherent» [31]

If two superconductors are separated by a thin insulating layer, then quantum mechanical tunneling can occur for the Cooper pairs without breaking up the pairs.

Good sensitivity of SQUID causes necessity of division between detection part and SQUID. Basic principle of measurement is to move a sample through detection coils. Current induced in detection system changes the magnetic flux. Superconducting shell plays significant role in screening external magnetic fields. Superconductive shield provides stabilization of existing magnetic field.

Pick-up coil system consists of three coils. Theoretically the sizes of coils should be similar, but practically the areas of coils always have small differences, and small magnetic disbalance exists. In case when sample has large magnetization, produced large currents can be a reason of noise in detection coils. Overall picture of different parts location near detection coils is drawn on Figure 1.5.5.

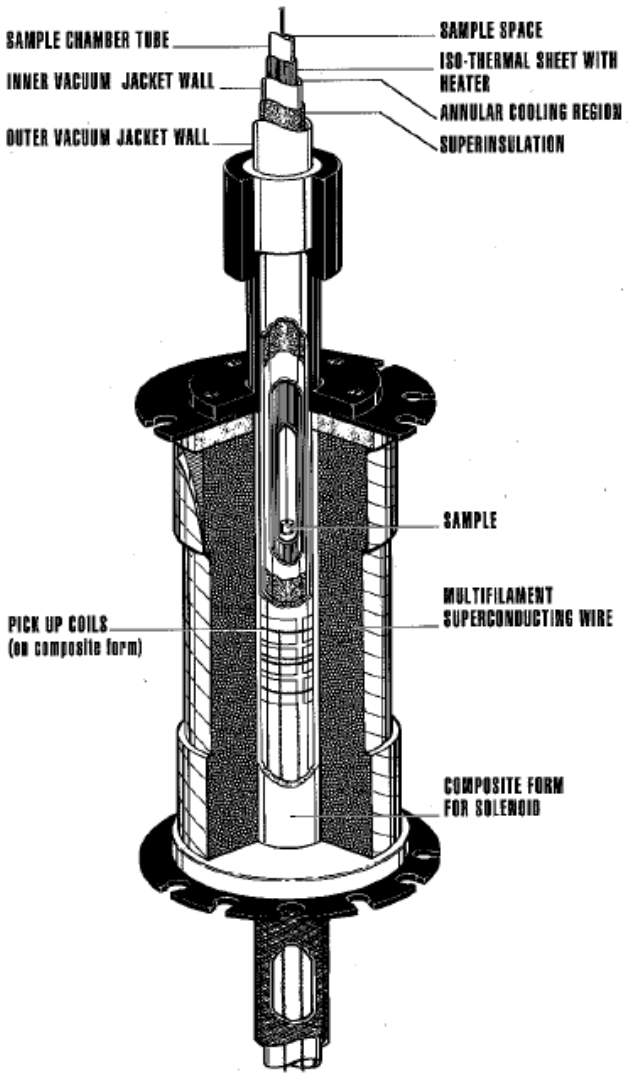

Figure 1.5.5. Location of detection coils and sample space [32].

Temperature control system is important part of system. It allows changing temperature of experiment.The temperature is controlled by two temperature sensors. Sensor A measures the temperature of the VTI heat exchanger and sensor B the temperature of the sample tube. Helium flow cools the sample and the controller's heater is used to control the temperature in the sample space. and temperature information is fed back to the temperature controller. The controller adjusts the heater's power to keep the temperature at a pre-adjusted value.

All central blocks which are used to maintain SQUID magnetometer functionality are drawn in picture 1.5.2. In left part of figure is shown overall photo of magnetometer construction, and in right side is drawn overall structure scheme.

2. Experimental.

2.1. Experiment conditions.

During experiments 5 samples (S11- S15) of nanotubes on polystyrene substrate.

Different oxidants were used in process of forge rolling synthesis of all samples: $K_2Cr_2O_7$ and $Na_2S_2O_8$, with adding of aniline. All samples has different content of iron: S11 sample contain of iron is 1 percent, S12 is 5 percent, S13 contain 2.5 percent, S14 contain 3 percent, and S15 is oriented nanotubes on silicon substrate.

All samples have been made by CVD technology using of force rolling method. After repeating of rolling process sample gets anisotropy in magnetic response. It can be connected with nanotubes orientation along direction of rolling.

For every sample magnetic-field and temperature dependences were measured. Each measurement point at certain temperature and magnetic field intensity was measured for several times for statistical purposes.

Magnetic-field dependence is a dependence of average internal magnetic moment on magnetic field. Temperature dependence is a dependence of average internal magnetic moment on temperature.

In measurement was special software was used for data acquisition. Main working window of this software is drawn in picture 2.1.1.

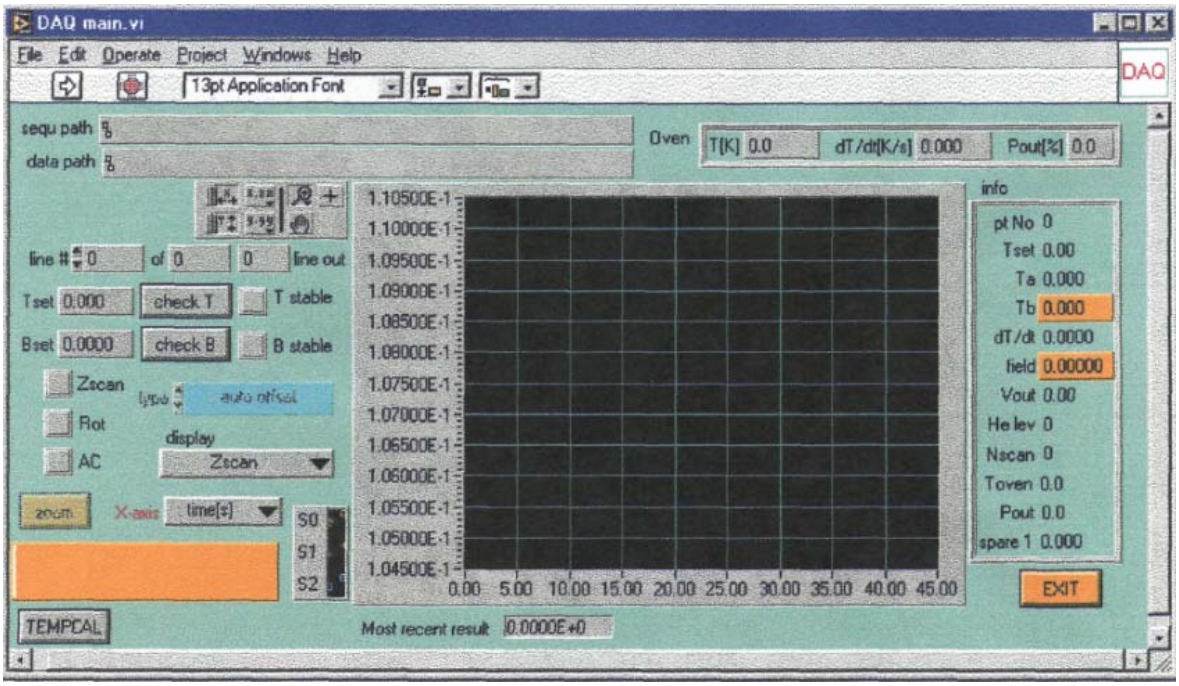

Figure 2.1.1. Main window of data acquisition software [33].

Measurements are performed by invoking the «Start Data Acquisition» function The user is prompted for a sequence file name and data storage file name, and optionally the sample mass, volume and a short description may be entered. Control is then transferred to the LabView subprogram «DAQ main.vi».

The «sequ path» and «data path» boxes show the file names of the sequence and data storage files. The «line» box shows the position in the sequence of the current measurement. The boxes «Tset» and «Bset» display the temperature and magnetic field set points for the present measurement respectively.

When measurement is done, the «line» point will advance and the temperature and magnetic field will be automatically adjusted to the values requested for the box «line». For each data point, either one of the AC and DC indicators will be highlighted according to the type of measurement being undertaken. The graphical display which forms the major part of the window displays the results obtained from the real time analysis of points in the sequence as they are calculated. This data may be plotted as a function of field and as a function of temperature. Toggling

between the two is achieved by clicking on the button to the left of the magnetic moment axis.

Testing for stability of the temperature and magnetic field can be toggled on and off by clicking on the buttons labelled «check T» and «check B», respectively. If the stability check for temperature or field is enabled then the appropriate indicator lights when the system detects that the configured stability criteria has been met.

2.2. Processing of experimental data, algorithm of removing bad data point.

A fragment of data which was obtained from SQUID data acquisition system is collected in Table 2.2.1.

For every magnetic field value average magnetic moment was obtained in process of automate measurement.

Table 2.2.1. A fragment of magnetic field dependence for S12 sample.

Number	Magnetic field [T]	average Moment [A]	scan#1	scan#2	scan#3	scan#4
1	0	1.99E-07	1.97E-07	1.96E-07	1.99E-07	2.03E-07
2	0.0167	2.51E-07	2.44E-07	2.51E-07	2.53E-07	2.57E-07
3	0.0373	3.04E-07	3.04E-07	2.94E-07	3.07E-07	3.13E-07
4	0.0572	3.63E-07	3.68E-07	3.57E-07	3.64E-07	3.62E-07
5	0.0771	3.98E-07	3.81E-07	4.13E-07	4.05E-07	3.92E-07
6	0.097	4.37E-07	4.24E-07	4.34E-07	4.55E-07	4.35E-07
7	0.1172	4.75E-07	5.06E-07	4.49E-07	4.51E-07	4.93E-07
8	0.1375	5.21E-07	5.03E-07	5.34E-07	5.05E-07	5.41E-07
9	0.1569	5.03E-07	5.14E-07	5.39E-07	5.54E-07	4.06E-07
10	0.1773	5.30E-07	4.41E-07	5.37E-07	6.15E-07	5.27E-07
11	0.1975	5.44E-07	4.87E-07	4.84E-07	5.90E-07	6.15E-07
12	0.2171	6.09E-07	6.23E-07	5.21E-07	5.32E-07	7.60E-07

Average moment column is calculated automatically as an average value of scan1-scan4 columns, which contain values of magnetic moment. This measuring principle of measurement allows to enhance the accuracy. Figure 2.2.1shows graph of magnetic field dependence for S12 sample at 3K temperature. Obtained dependence contains a lot of bad data points. Reason of their existence is errors in proccess of computerized calculation, due to SQUID signal drift.

During the processing of experimental results algorithm for deleting bad data points was developed. It is based on comparison of every «scan(№)» value of internal magnetic moment with their average value. If «scan (№)» value differs

from average moment more than 30 percent, then it is equated to zero and is eliminated from calculations. This way new graphs were built.

Mathematical principles of processing are stated below.

First step is to calculate selective dispersion:

$$S_x = \frac{\Sigma(\bar{x} - x_i)^2}{N} \qquad (2.2.1).$$

where $\bar{x}$ is an average value of internal magnetic moment of sample, measured in each scan, x_n is magnetic moment measured in each scan, «N» is a number of scans.

Next step in bad data points removing algorithm is calculation of standard deviation:

$$S(x) = \sqrt{S(x^2)}\,. \quad (2.2.2)$$

Then acceptance error is estimated for chosen value of acceptance probability. Let consider level of acceptance probability 70 percent. With help of Student coefficient table the value of probability is 1,4579 for amount of measurements

N= 6:. At this value all «bad» data points which has big discrepancy with average value, are removing.

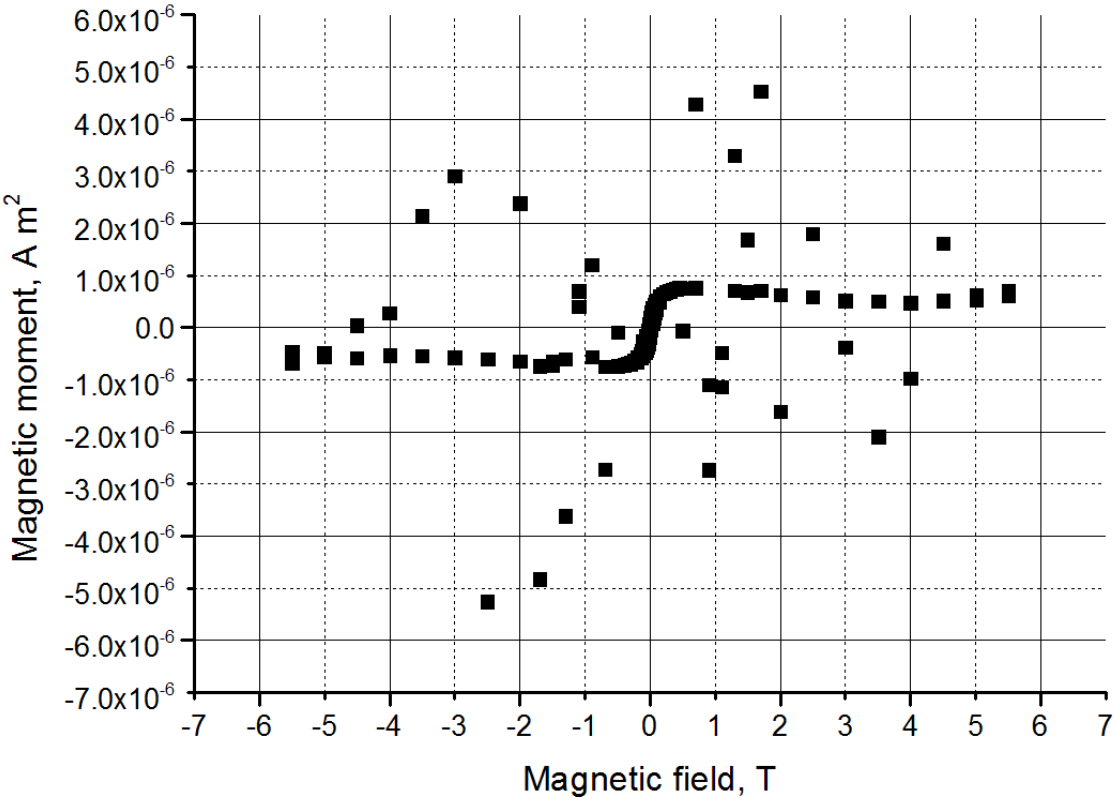

Figure 2.2.1.Magnetic field dependence for S12 sample at temperature 3 K before processing by algorithm of removing bad data points.

Figure 2.2.1 shows big dispersion of points. It complicates the understanding of the magnetization curve. After application of algorithm graph changes drastically. The new result is the presented in Figure 2.2.2.

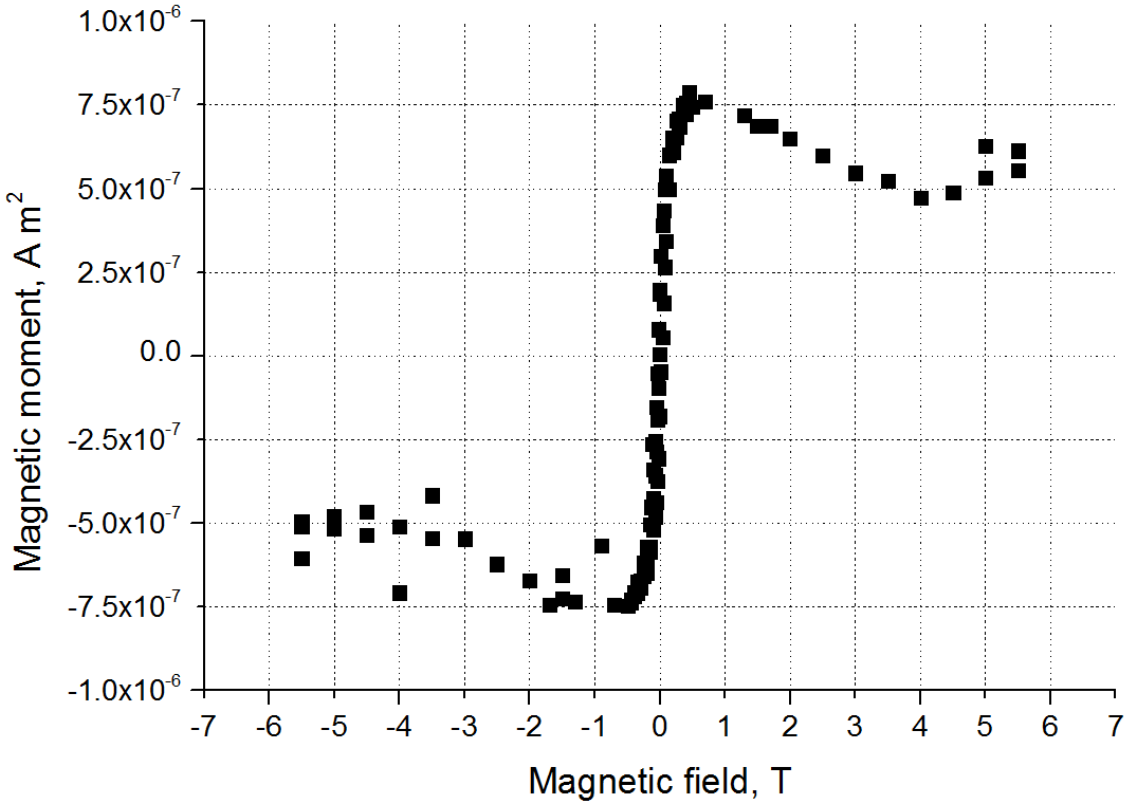

Figure 2.2.2.Magnetic field dependence for S12 sample at temperature 3 K after deleting of bad data points.

Used algorithm has some disadvantages. If most part of scans in one measurement has significant difference with the average value, then the average magnetic moment can be determined in incorrect way. Such data points require manual correction. Finally such correction increases the time of processing.

2.3. Magnetic field dependences of samples magnetization.

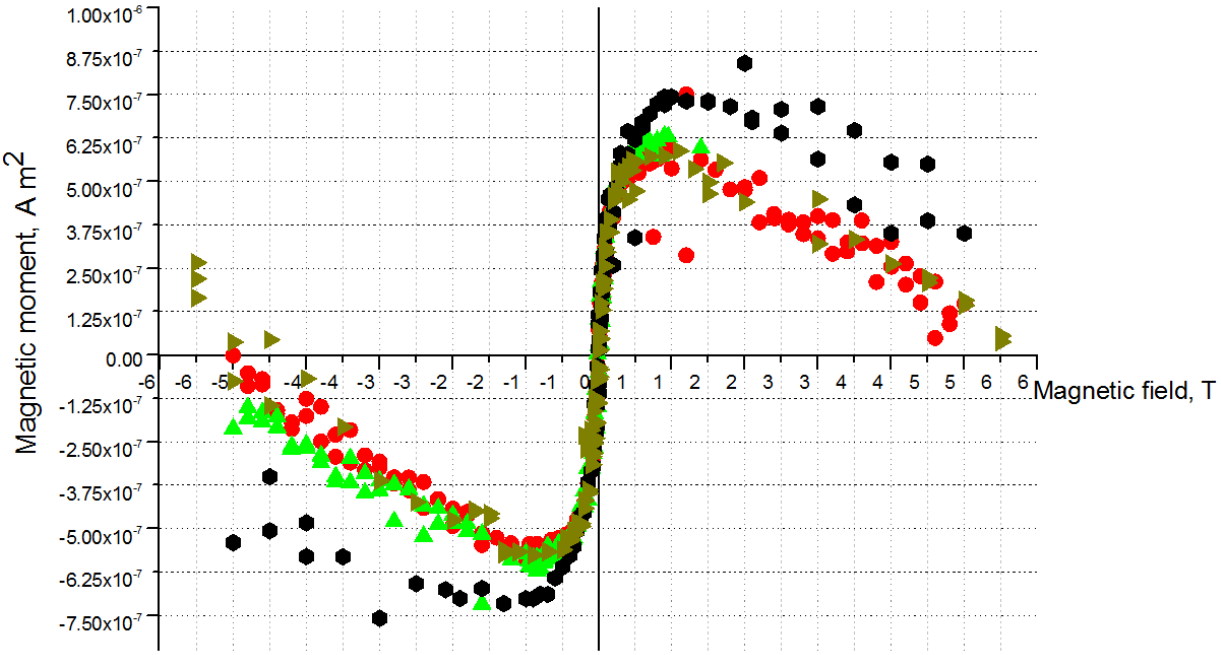

Figure 2.3.1 Magnetic field dependence for S11 sample at different temperatures 3K 15K 50 K 150 K 300 K.

Fig. 2.3.1 shows magnetization curves of the sample S11 at temperatures of 3 K, 50 K, 150 K and 300 K. All of the curves show the typical hysteresis loop of a ferromagnetic material, but in chosen scale loop is not visible well. Hysteresis became more noticeable at the low temperatures. Both the saturation magnetization and the coercivity increase as temperature decreases.

In area where magnetic field intensity has negative value, increasing of temperature results to more high location of curve. Saturation is achieved at the intensity of magnetic field about 0.5 T. After this point big decrease of dependences can be observed.

This increase in coercivity of the carbon nanotube upon incorporation into the composite may well be the result of interfacial couplings between the SWCNTs and polystyrene.

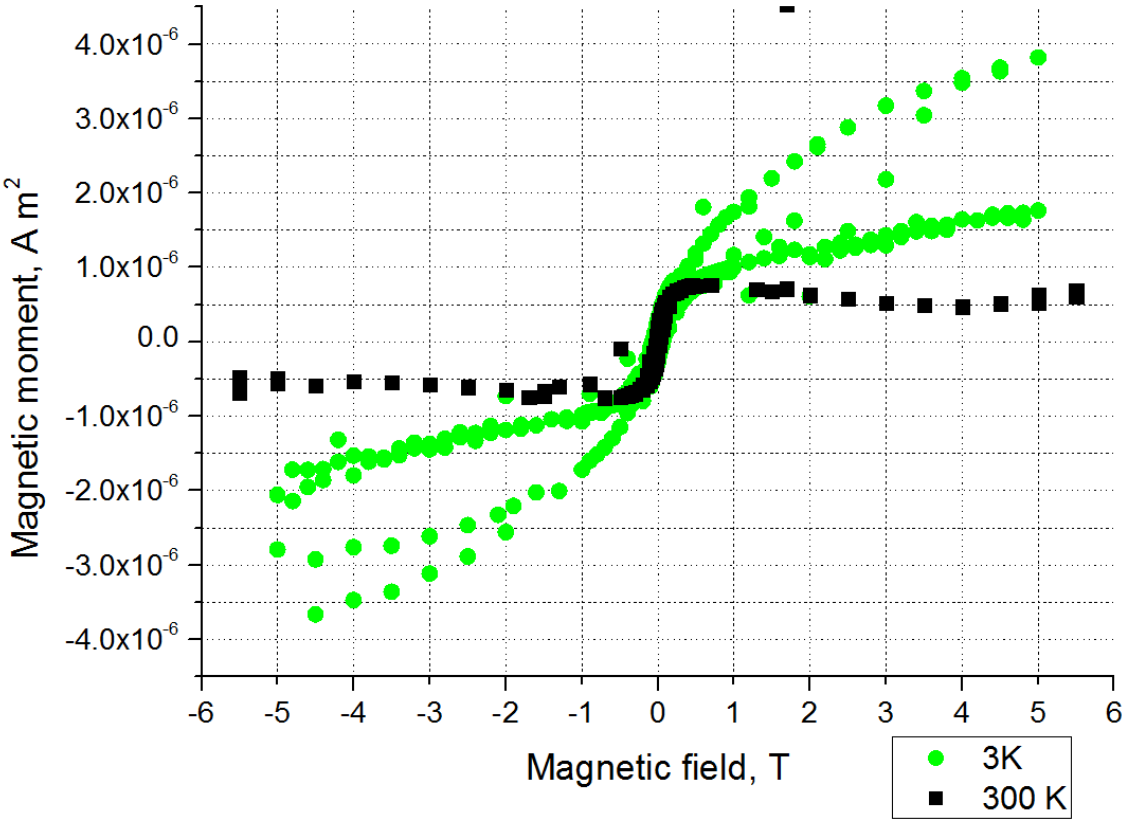

Figure 2.3.2 Magnetic field dependence for S12 sample at 3 and 300 K temperatures.

All magnetization curves have parts of linear increase of magnetic moment with extension of temperature. For sample S12 this sites situated when intensity of a magnetic field accepts values from -0.6 T to 0.6T, as shown in Figure 2.3.2 Part of linear growth can be characterized by angle of tilt angle. This angle is not the same for different temperatures. In Figure 2.3.2 is clearly shown, that the enhancement of temperature results to reducing of tilt angle for linear growth part.

Iron nanoparticles has significant contribution in magnetism. Concentration of particles closely connected with magnetization of sample. It especially noticeable for part of linear growth. It allows to make conclusion that at high temperatures

contribution of iron nanoparticless in ferromagnetic behavior became less significant, because tilt angle of linear part reduced.

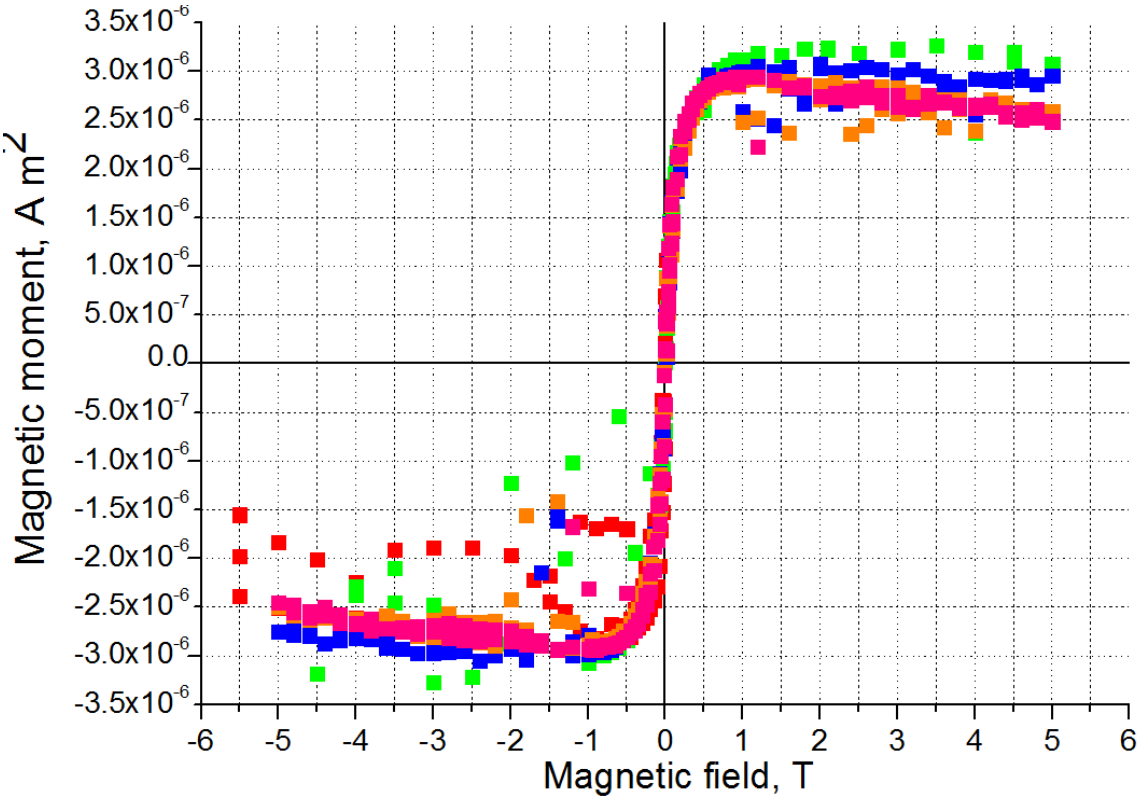

Figure 2.3.3 Magnetic field dependence for S13 sample for temperatures 3 K 15 K 50 K 150 K 300 K.

In figure 2.3.3 shown that after saturation achieved at intensity of magnetic field 0,5 T, part of constant magnetization can be observed. It means that polystyrene substrate not has contribution in magnetization.

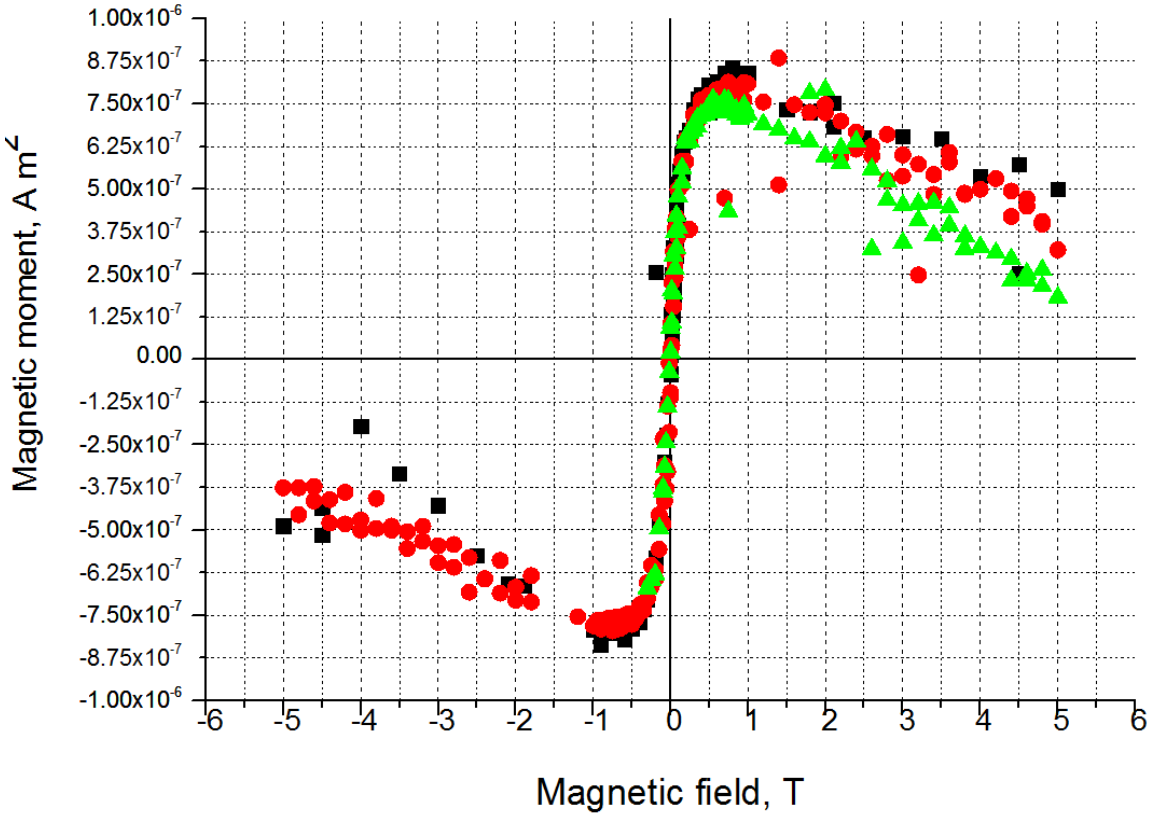

Figure 2.3.4.Temperature dependence for S14 sample temperatures ■ 3 K, ● 15 K, ▲ 50 K.

Magnetic contribution of polystyrene substrate can be shown in Figure 2.3.4, because significant reducing of magnetic moment can be observed at intensities of magnetic field from -4T to 0 T , and from 1 T to 5 T .

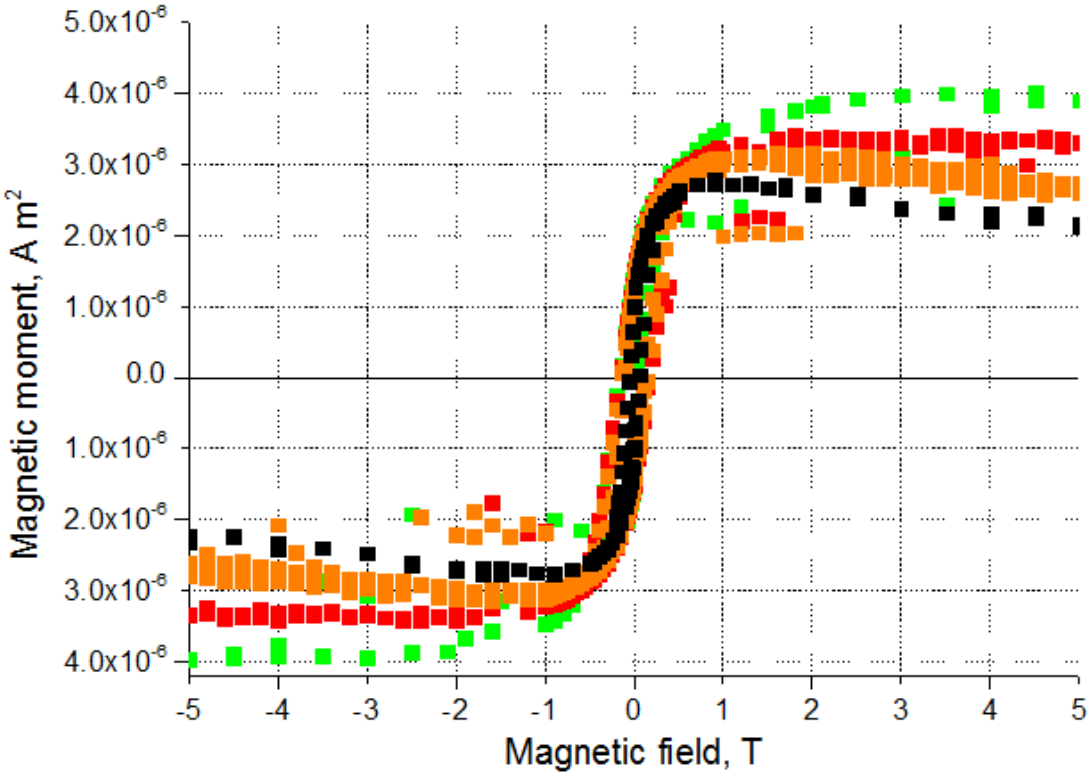

Figure 2.3.5 Magnetic field dependence for S15 sample in temperature range 3 -300 K: 3K 15 K 50 K 300 K.

For sample S15 small tilt angels for linear parts is shown in Figure 2.3.5. It can be explained by low content of iron in sample.

2.4. Temperature dependences of magnetization.

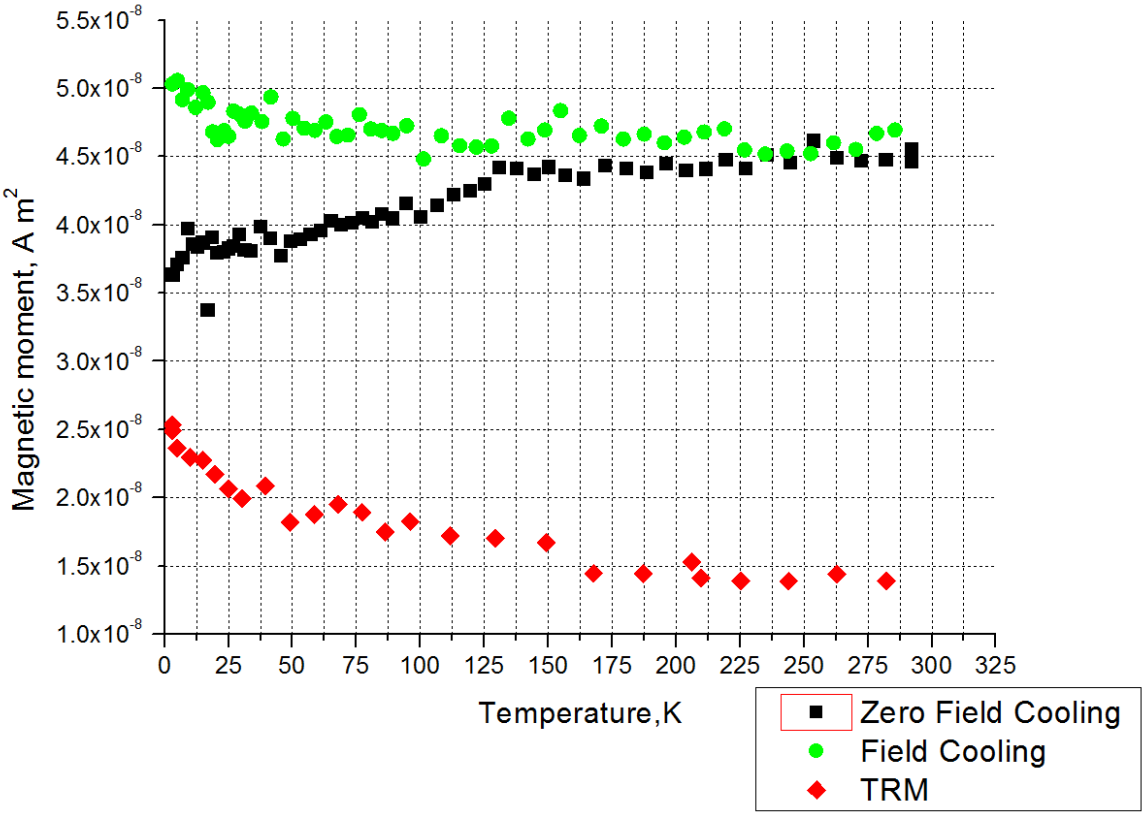

Figure 2.4.1 Temperature dependence for S11 sample.

Investigation of temperature dependences for all samples was done in three different regimes: Zero Field Cooling (ZFC), Field Cooling (FC) and Thermoremanent regime (TRM). Scheme of sequence of these regimes is shown in Figure 2.4.2.

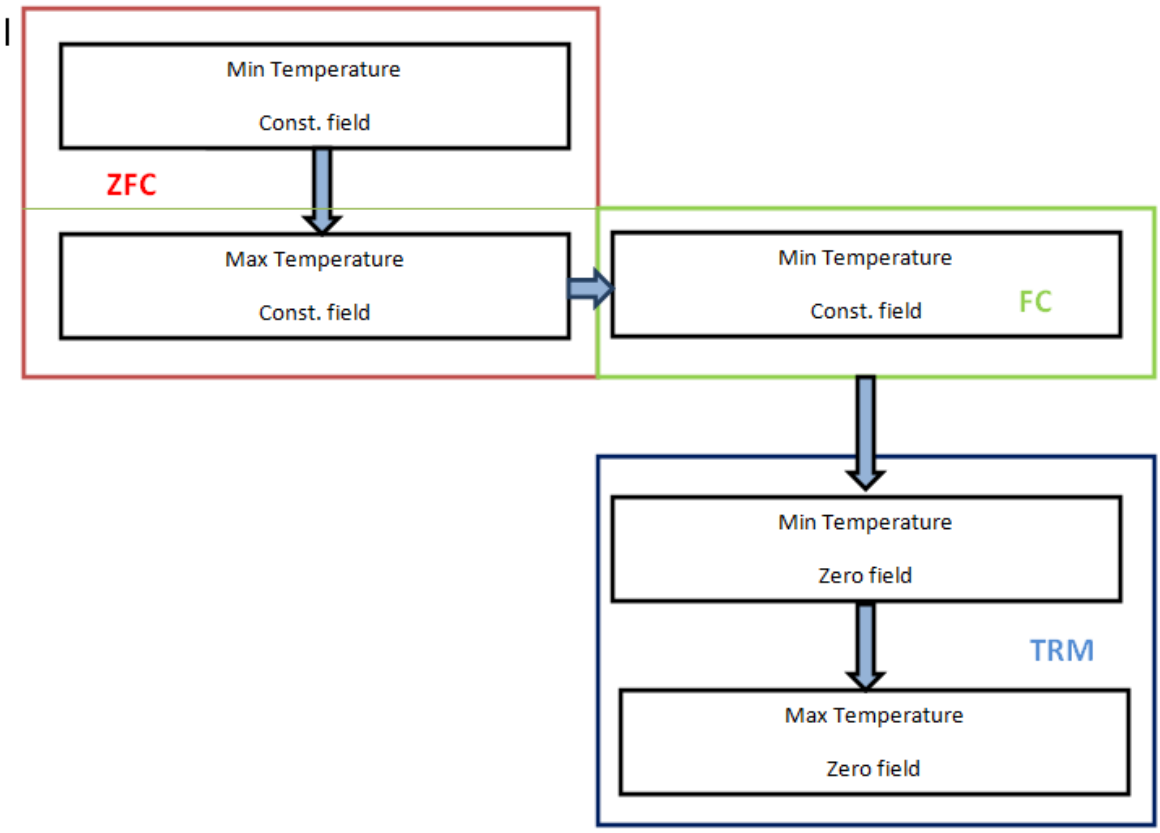

Figure 2.4.2 Overall scheme of sequence of regimes in process of measurement.

Zero field cooling regime assumes that the sample is cooled down to the lowest temperature in zero magnetic field, then certain magnetic field is turned on. Sample space is heated step by step to 300 K. Next regime is field cooling with gradual reducing of temperature. Thermoremanent regime is characterized by heating of sample in zero magnetic field with after cooling in field.

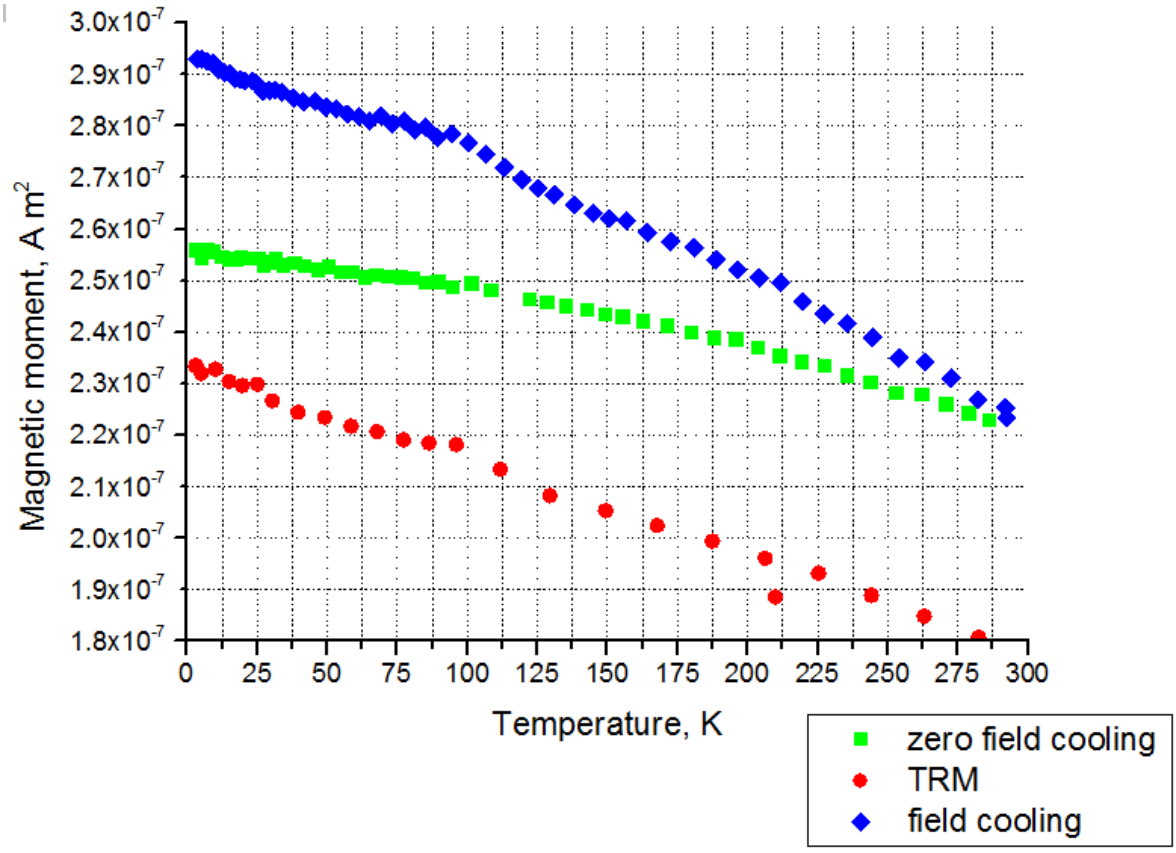

Figure 2.4.3 Temperature dependence of magnetization of S12 sample, external field B=100 G.

Magnetic-temperature dependence has contradiction with molecular field theory, that predicts constant magnetization when temperature getting equal zero [34].

Below certain temperature ZFC decreases during heating while FC continues to increase when temperature decrease[35]. It can be explain content of iron in sample.

Magnetic properties of polystyrene substance have not very big influence on temperature dependence. Polystyrene displayed small magnetic response. This response can be estimated on magnetic field dependences as a small inclination. In cases of measured samples such inclination practically unnoticeable in obtained dependences.

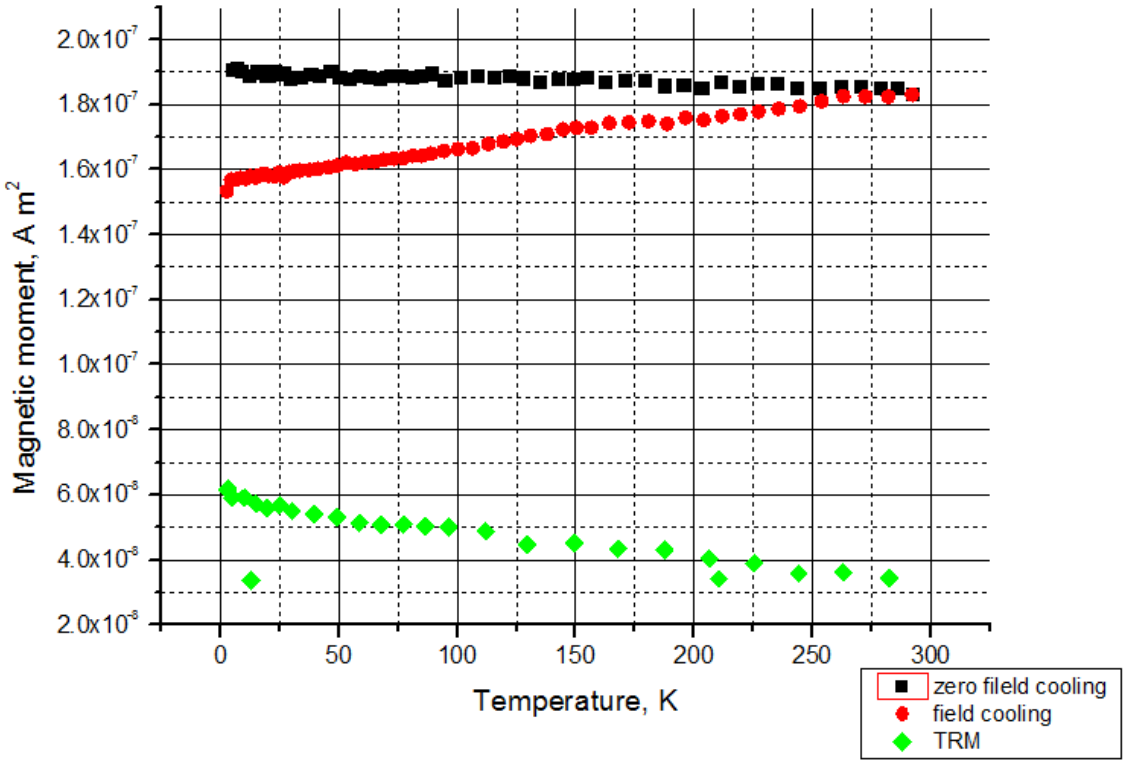

Figure 2.4.4.Temperature dependence of magnetization for S13 sample at field 100 G.

Temperature dependence of magnetization of S15 sample has some unusual feature. S15 sample contain massives of high oriented nanotubes on silicon subtrate, formed by CVD method. Rolling of nanotubes, which is repeated many times during synhtesis, can be reason of magnetic response anisotropy. Decreasing characrter of magnetization in condition of zero magnetic field (ZFC mode) caused by magnetic anisotropy. Technological features of CVD method also has influence on non-typical behaviour of the curve in this regime.

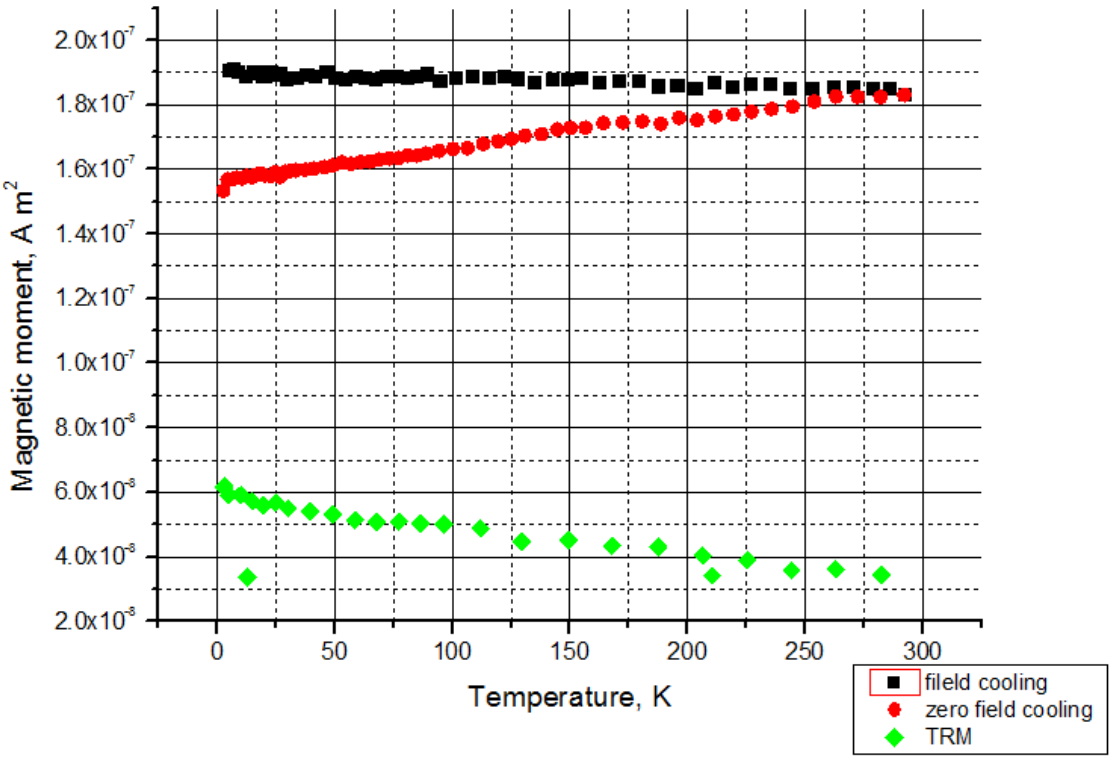

Figure 2.4.5. Temperature dependence for S14 sample, magnetic field 100 G.

In process of synthesis of sample S14 Ni catalyst was used. It suggests existence of magnetic anisotropy of Ni, which can be contained in nanotubes. In absence of magnetic field blocked state was observed, but if magnetic field is applied, energetic and thermal barrier will overcome, and features of superparamagnetic behavior can be shown [36].

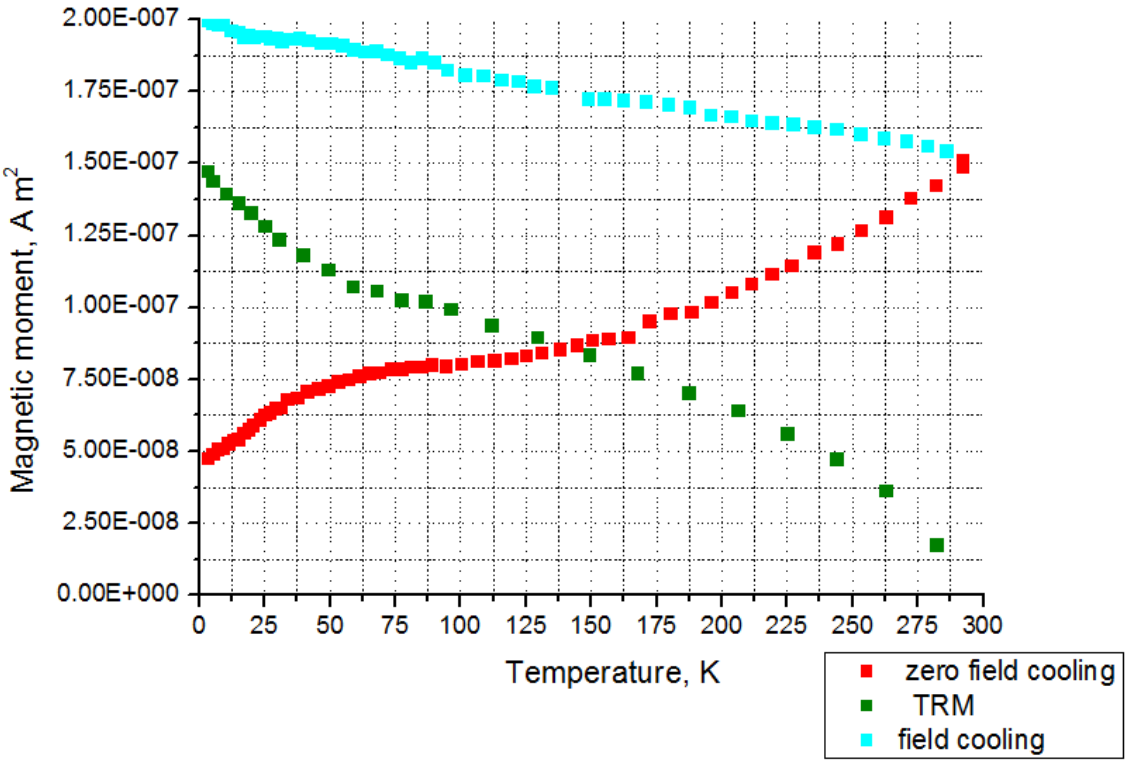

Figure 2.4.6.Temperature dependence for S15 sample (100 Gauss external magnetic field)

2.5. Atomic-force microscopy investigations.

For successful observation of nanotubes resolution 10 nm of microscopy is needed, because the nanotubes have characteristic length of has value of 10 nm and the width less than 10 nm.

Atomic force microscopy has sufficiently good perspectives to obtain of detailed images of nanotubes. During the work surface morphology images were obtained for samples S11, S12, S13, S14, S15.The resolution of the AFM allows one to see the heterogeneities and defects of the nanotubes especially it was noticeable for S12 sample.

Figure 2.4.1. «Bruker MultiMode 8» microscope [37].

In this work AFM microscope «Bruker MultiMode 8» was used. The high-speed scan system of microscope enables to make fast scanning of samples. A large variety of standard operating modes and many unique capabilities enable the AFM system to characterize mechanical and electrical properties of samples. Also possibility to make heating of investigated samples is presented; available temperature interval is from -30 to 250 degree.

According to the photo, all nanotubes lay in one horizontal plane. It is an evidence for existence of horizontal-oriented nanotubes obtained in result if forge rolling along long side of composite.

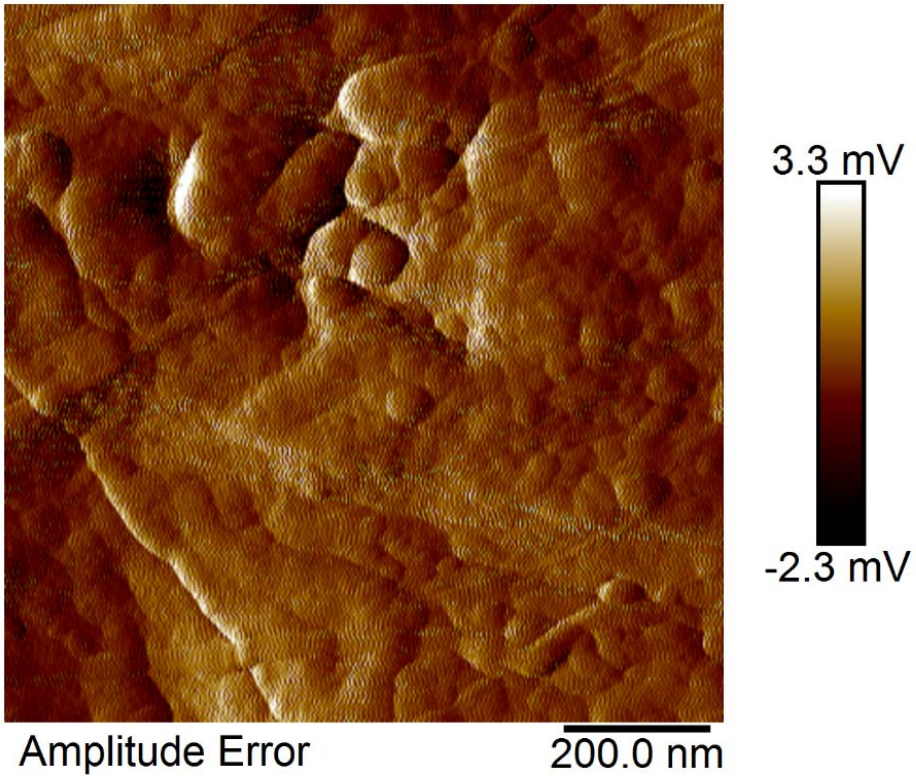

Figure 2.4.2 Pictures of sample S12 surface with nanotubes .5 percent of iron in sample.

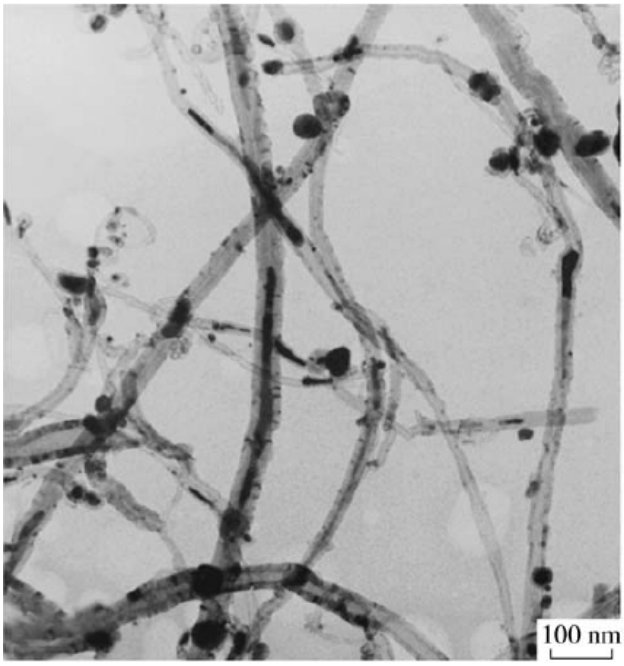

Figure 2.4.3. TEM images of CNTs with encapsulated iron nanoparticles [38].

Possibilities of transmission electron microscopy (TEM) allows one to investigate metallic nanoparticles inside nanotubes. Moreover, existence of defects and particles can be registered by the reduction of magnetic anisotropy [39].

The maximal macroscopic magnetic anisotropy energy in a system of nanotubes filled with iron nanorods theoretically can be estimated as $8 \cdot 10^6$ erg/cm However, imperfect nanotube structures and array texture lead to a decrease in the macroscopic magnetic anisotropy energy $0.9 \cdot 10^6$ erg/cm [40].

Conclusion

During scientific work magnetic properties of carbon nanotubes on polystyrene substrate were investigated using SQUID magnetometer. Samples with the high concentration of iron were examined using AFM.

Magnetic properties o f samples depend on contribution not only nanotubes but on substance. Contribution of polystyrene substrate is shown on obtained magnetic field dependences, especially it noticeable for S13 sample. Also nanoparticels of iron has influence on magnetic behavior of samples. Magnetic influence of iron nanoparticles in magnetic properties became less significant with temperature increase.

For processing of the experimental data algorithm was developed. It allows to exclude bad data points and filter the data. The algorithm is based on comparison of points with average value, allowing to select and delete bad points caused by instrumental errors.

Temperature dependences of magnetization for all samples were investigated. Unusual character of temperature dependence for S15 sample can be explained by existence of magnetic anisotropy occurred during CVD method of synthesis.

Investigation of multi-walled nanotubes with help of atomic-force microscopy in case of sample S12 with 5 percent content of iron give visualization of contours of nanotubes under polystyrene layer.

References.

1. The electronic properties of graphene and carbon nanotubes.
[Acessed 11 April 2014]. Available at
http://www.nature.com/am/journal/v1/n1/fig_tab/am200923f1.html

2. F.Lu et al., Chem. 2010.Phys.ics Lett. 497, p.57.

3. Physics Uni portal . [Acessed 27 April 2014]. Available at http://www.phys.uni-sofia.bg/~vpopov/elbscomp.htm.

4. Nanotubes make perfect diodes.Physics World magazine.2005.
[Acessed 27 April 2014].Available t http://c-12.falm.me/ntrubki.svoistva.html

5. NRAM technology.2013. NRAM Practical Application. [Accessed: 15 April 2014]. Available at http://www.nantero.com.

6. Future of nanotube.Computer Press. [Accessed 21 March].Avaliable at http://compress.ru/.

7. Practical properties of nanotubes.2011. [Accessed 28 April 2014]. Available at http://www.c-12.falm.me/

8. NRAM technology. Accesed [Accessed 21 April 2014]. Available at http://www.nantero.com

9. NRAM application technology. [Accessed 14april 2014]. Available at http://www.nantero.com.

10. M. Terrones, N. Grobert, J. Olivares, et al.1997.Nature (London) 388, p.52 .

11.Iijima S. Helical microtubules of graphitic carbon . 1991.Nature. V. 354. P.56.

12. Kosakovaskya Y. Nanofibre carbon strucure . 1992. Letters to Journal of Experimental and Theoretical Physics . V. 56. p. 26

13. Rigaku Mechatronics. 2014. [Accessed: 26 Mart 2014].Available at http://en.rigaku-mechatronics.com/case/arc-discharger.html.

14. Wondrous world of carbon nanotubes. [Accessed:23 March 2014]. Available at http://students.chem.tue.nl/ifp03/synthesis.html.

15. Arrays of Carbon Nanotubes Aligned Perpendicular to the Substrate Surface: Anisotropy of Structure and Properties ,A. V. Okotrub L. G. BulushevaA. G. KudashovV. V. Belavin.
16. Preparation of Carbon Nanotubes by CVD Process over Nanoparticles of Ni-Ce-Zr Mixed Oxides. 2008. F. Farzaneh, N. Faal Hamedani and V. Daadmehr. Journal of Sciences, Islamic Republic of Iran 19(2): 119-123.

17. Magnetic solids [Accessed 11 April 2014]. Available at. http://www.just.edu.jo/~aobeidat/PDF/research/Ferrofluids/Ferromagnetic.pdf
18. Solids – Superconductors and Magnetic Properties. [Accessed 11 April 2014]. Available at http://www.public.iastate.edu/~adamkam/teaching/phys322_S09
19. Web resource NDT Resource Center, [Accessed 21 April 2014]. Available at www. ndt-ed.org.
20. Web resource NDT Resource Center, [Accessed 21 April 2014]. Available at www. ndt-ed.org.
21. Variety of types of magnetic ordering. Progress of physical sciences, February 1984 Vol. 142, Part 2
22. Variety of types of magnetic ordering. Progress of physical sciences, February 1984 Vol. 142, Part 2
23. Makarova, T.L. 2004 Magnetic properties of fullerenes.Moscow.
24. Doping and the unqiue role of vacancies in promoting the magnetic ground state in carbon nanotubes and C_{60} polymers. 2006.Antonis N. Andriotois, R. Michael Sheetz. Physical Review B 74 .
25. McConnel .Model for the Magnetism of C6o-based Polymers, A.N. Andriotisa, M. Menonb, R. M. Sheetz0, and E. Riehterd.
26. O.E. Kvyatskovskii, I.B. Zakharova., A.L. Shelankov, T.L. Makarova.2005.Fullerene and Nanotubes.
27. G.M. Zhao and Y.S. Wang. 2006.Trends in nanotubes Research. New York, pp.39-75.

28. Go meng Ghao, Pieder Beeli.2008.Observation of an ultrahigh-temperature ferromagnetic-like transition in iron. Physical Review Vol.77.
29. Hyperphysics, [Accessed 2 May].Available at http://hyperphysics.phy-astr.gsu.edu.
30. Hyperphysics, [Accessed 2 May].Available at http://hyperphysics.phy-astr.gsu.edu.
31. Hyperphysics, [Accessed 2 May].Available at http://hyperphysics.phy-astr.gsu.edu.
32. Mike Mcelfresh. 1994.Fundamentals of magnetism and magnetic property measurement system. Purdue University. West Lafayett.
33. S600 Squid susceptometer operational manual.
34. Nicola A. Spaldin.2010.Magnetic Materials: Fundamentals and Applications.2th ed University of California.
35. Bai, X; Son, SJ; Zhang, SX; Liu, W; Jordan, EK; Frank, JA,etc. 2009.Synthesis of superparamagnetic nanotubes as magnetic resonance imaging contrast agents. and for cell labeling. Nanomedicine Vol.3: 163-174.
36. Nicoleta Lupu.2010.Magnetic Properties of nanowires guided by carbon nanotubes. Nanowires Science and Technology.
37**.** «Bruker MultiMode 8» manual.
38. Mei Li Erik Dujardin and Stephen Mann**.** Programmed assembly of multi-layered protein/nanoparticle-carbon nanotube conjugates. 2005. Chem. Commun., 2005, 4952-4954.
39. Teri Wang Odom. Jason Hafner Charles M. Lieber. 2008.Scanning Probe microscopy studies of carbon nanotubes.
40. Arrays of Carbon Nanotubes Aligned Perpendicular to the Substrate Surface: Anisotropy of Structure and Properties ,A. V. Okotrub L. G. BulushevaA. G. KudashovV. V. Belavin.